BIOFILMS MEDIATE THE PRESERVATION OF LEAF ADPRESSION FOSSILS BY CLAYS

Authors: LOCATELLI, EMMA R., McMAHON, SEAN, and BILGER, HANS

Source: PALAIOS, 32(11) : 708-724

Published By: Society for Sedimentary Geology

URL: https://doi.org/10.2110/palo.2017.043

PALAIOS
Emphasizing the impact of life on Earth's history

PALAIOS, 2017, v. 32, 708–724
Research Article
DOI: http://dx.doi.org/10.2110/palo.2017.043

BIOFILMS MEDIATE THE PRESERVATION OF LEAF ADPRESSION FOSSILS BY CLAYS

EMMA R. LOCATELLI,[1,2] SEAN McMAHON,[1,3] AND HANS BILGER[1]
[1]*Department of Geology and Geophysics, Yale University, P.O. Box 208109, New Haven, Connecticut, 06520-8109, USA*
[2]*1150 4th St. SW, Washington D.C. 20024, USA*
[3]*UK Centre for Astrobiology, School of Physics and Astronomy, University of Edinburgh, EH9 3FD, UK*
email: sean.mcmahon@ed.ac.uk

ABSTRACT: **Leaf adpression fossils vary in their organic content, relief, and quality of preservation. Some of the most enigmatic adpressions, known as leaf molds, retain fine morphological and anatomical details despite being found in coarse sandstones—a widespread phenomenon attributed to the presence of fine-grained minerals on the fossil surface. Previous taphonomic studies have demonstrated the importance of microbial biofilms in promoting mineralization and argued that authigenic iron oxides can serve as the preserving medium. Here, we propose that this role is played more commonly by biologically precipitated aluminosilicate phases (clays). To test this hypothesis, we conducted energy dispersive X-ray spectroscopy (EDS) analysis of thin sections through fossil leaves from five localities differing in age and depositional environment. Point spectra taken directly from the leaf-sediment interface revealed that cation-rich clays separate the leaf fossils from the matrix. Additional EDS analyses of biofilms on a fossil leaf and on modern oak leaves decaying in freshwater also revealed aluminosilicates, for which we infer a biofilm-mediated, authigenic origin. These results are the basis of a novel 'Biofilm-Clay Template' taphonomic model, whereby microbially mediated clay authigenesis is commonly the first step in leaf adpression preservation.**

INTRODUCTION

Leaves are common fossil plant organs. The majority of fossil leaves are preserved as "adpressions", a style that encompasses a spectrum from carbonaceous, nearly two-dimensional films ("compressions"; Fig. 1A–1D) to organic-poor, somewhat higher-relief "impressions" of the leaf lamina and veins (Fig. 1E–1H) (Shute and Cleal 1986). Such leaf adpression fossils (LAFs) retain a range of morphological and anatomical details and vary in their organic content from compressions that include well-preserved organic cuticles to impressions that lack organic remains entirely (Locatelli 2014). Three-dimensionally preserved leaves with little organic matter may be referred to as molds rather than impressions (e.g., leaves from the Dakota Sandstone, Fig. 1F–1H).

Paleobotanists have long recognized that LAFs, including some that lack organic matter, can retain surface details (e.g., venation, trichome bases) on a finer scale than the grain size of the surrounding matrix (usually sandstone) because of the presence of a fine-grained mineral coating (e.g., Schopf 1975; Fig. 1). LAFs are also commonly distinguishable from their surrounding matrix by color (e.g., Fig. 1B, 1D, 1E) or by the regular orientation of clays parallel to the leaf surface, which contrasts with the random orientation of matrix grains (e.g., Mamay 1989, fig. 2). The widespread occurrence in both time and space of LAFs with a fine-grained mineral coating and a color that contrasts with the matrix suggests a common process. One of the long-standing problems in paleobotany has been determining the mechanism(s) responsible for these phenomena and explaining the formation of different forms of leaf adpressions represented in the fossil record.

In a pioneering paper, Spicer (1977) sought to address these phenomena by comparing modern leaves decaying in a freshwater stream and delta with a fossil leaf from the Cretaceous Dakota Sandstone that displayed fine details in a coarse matrix. Energy dispersive X-ray spectroscopy (EDS) showed that a thin layer of iron oxides, with small amounts of aluminosilicates, had formed on the modern leaves within weeks of submersion. The Dakota Sandstone leaf surface was highly enriched in iron, while the matrix away from the fossil contained a mixture of both iron and silicon. Spicer therefore proposed that the fine details in some fossil leaf impressions result from the precipitation of authigenic iron on the leaf surface soon after entry into a depositional environment, and suggested a microbial mineralization pathway. Dunn et al. (1997) produced experimental support for this hypothesis by immersing leaves with and without bacterial biofilms (dense, laminated populations of cells embedded in extracellular polymeric substances, EPS) in aqueous $FeCl_3$. Ferrihydrite precipitated within ten minutes, but only on the biofilm-covered leaves, implying that precipitation resulted from the adsorption of iron to bacterial EPS. However, these experiments were conducted at very high concentrations of $FeCl_3$ (nine times higher than even the most iron-laden water in a metal-contaminated acid lake; Ferris et al. 1989), which would have artificially encouraged precipitation and inhibited bacterial decay, while other cations that would naturally compete with iron (e.g., Al^{3+}, Mg^{2+}) were not tested.

Although the conclusion that microbial biofilms contribute to the mineral coating of fossils is consistent with experiments and fossil analyses of other soft-bodied organisms (Briggs 2003), many fossil leaves confirmed to be preserved in biofilms show no evidence of associated iron oxides (e.g., Harding and Chant 2000; Allison et al. 2008; O'Brien et al. 2008), indicating that iron oxide enhancement of fossil leaf preservation is not universal, and probably depends on iron availability. An alternative and complementary taphonomic explanation for the preservation of leaf impression fossils is suggested by studies of the taphonomy of some Ediacaran soft-bodied organisms, which are preserved in close association with microbially mediated clay minerals, either as impressions in sandstones (e.g., *Aspidella*, Laflamme et al. 2011) or compressions in shales (e.g., *Shaanxilithes*, Meyer et al. 2012).

The purpose of this study is to test the hypothesis that the microbially mediated authigenesis of clays may be responsible for enhanced

Published Online: November 2017
 0883-1351/17/032-708/$03.00

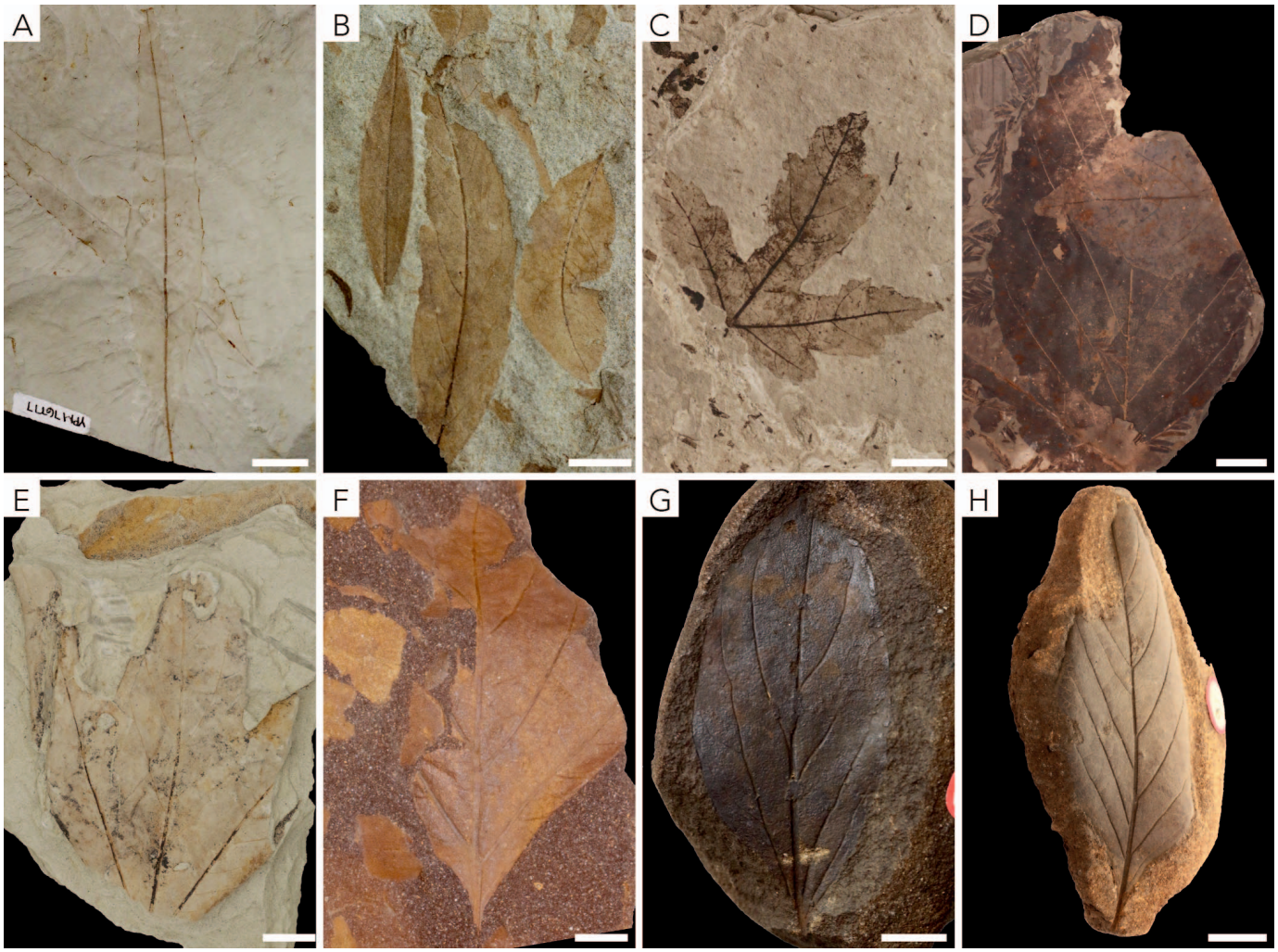

FIG. 1.—Examples of fossil angiosperm leaf adpressions from the Yale Peabody Museum of Natural History (YPM). **A**) Golden Valley Formation, Eocene, YPM 76777. **B**) Hell Creek Formation, Cretaceous, YPM 7831. **C**) Florissant Formation, Oligocene, 28356. **D**) Fort Union Formation, Paleocene, YPM 8336. **E**) Hell Creek Formation, Cretaceous, YPM 6475. **F**–**H**) Dakota Sandstone Formation, Cretaceous, YPM 25129, 55693, 168195. All scale bars = 1 cm.

preservation of fine-scale details in some fossil leaf compressions. Our aim is to provide the first documentation of the arrangement, texture and elemental composition of the fine-grained minerals found on the surface of several different fossil leaf impressions preserved in a wide variety of environments. We analyzed thin sections made transversely through leaf adpression fossils from five North American localities using EDS point analyses to determine the elemental composition of minerals directly along the leaf-sediment interface and in the matrix. We compared these data to elemental analyses of biofilms preserved on a fossil leaf and biofilms formed on a modern oak leaf decaying in the laboratory after 20, 45, and 100 days of decomposition. Our findings confirm the importance of microbial biofilms in non-mineralized tissue preservation, and form the basis of a new taphonomic model to explain the preservation of intricate details on fossil leaf surfaces.

MATERIALS AND METHODS

Fossil Leaves

Six fossil leaf-bearing specimens from five North American floras (Table 1; full descriptions below) were selected for thin section analysis on the basis of the visible presence of leaves entombed within the matrix (evident as carbon films between laminae). As the leaves are only visible in thin section, they cannot be assigned to specific taxa. The floras are Cretaceous to Oligocene in age and represent a range of fluvial, lacustrine, and floodplain settings. Four of the localities (five leaves, two from the Dakota Sandstone) were selected on the basis of previous reports and personal observations of leaf preservation in the localities as impressions coated by fine-grained minerals to allow additional comparisons with the analyses presented by Spicer (1977).

One organic-rich sample from the Fort Union Formation, North Dakota, was selected for its compression fossil content as a contrast to the impression fossils from the other localities. A small fragment ($< 10 \times 10$ mm^2 area) with a fossil angiosperm leaf preserved on its surface was selected to assess the possible preservation of fossil biofilms, which have been found on other compression fossils (e.g., McLean et al. 1999). The leaf tissue was black and continuous, indicating organic preservation. All samples were from the collections of the Division of Paleobotany in the Yale Peabody Museum of Natural History (YPM).

Dakota Sandstone Flora (Dakota Group, Kansas).—The two specimens (YPM 26713; YPM 25365) are from the lower Cenomanian (93.0–98 Ma; Ravn and Witzke 1994) Dakota Group (popularly referred to

TABLE 1.—*Summary of EDS analyses for each of the thin sections. The tallies presented in the Iron and Cation columns refer to the EDS spectra presented in Figures 2–7. Abbreviations: LSI = Leaf-sediment interface; K = Cretaceous; PC = Paleocene; EO = Eocene; OL = Oligocene; IMP = Impression; COM = Compression.*

YPM No.	Flora	Age	Setting	Mode	Major Peaks		Minor Peaks		Iron		Cations	
					Matrix	LSI	Matrix	LSI	Matrix	LSI	Matrix	LSI
27613	Dakota Sandstone	K	Fluvial	Mold	Fe, O	Si, Al, O	Si, Al	Fe, K, Mg, K, Ca	2/2	3/4	—	4/4
25635	Dakota Sandstone	K	Fluvial	Mold	Fe, O	Si, Al, Fe, O	Si, Al	Na, K	2/2	4/5	—	2/5
8384	Hell Creek	K	Fluvial	IMP	Si, O, Al, Fe	Si, Al, O,	Mg, Ca, Na, K	Ca, Fe, Mg, K	1/2	3/5	2/2	4/5
8336	Fort Union	PC	Pond	COM	Si, O, Al	Si, Al, O	—	Mg, Ca, Na, K, Fe	—	1/5	—	5/5
5595	Republic	EO	Lake	IMP	Si, O, Al	Si, Al, O	Na, Ca	Na, Mg, K	—	—	2/2	5/5
23724	Florissant	OL	Lake	IMP	Si, O, Al	Si, Al, O	—	Mg, Ca, Na	—	—	—	5/5

as the Dakota Sandstone), a loosely defined succession deposited in fluvial, floodplain, and coastal environments during transgressive phases along the eastern margin of the Western Interior Seaway from Minnesota to Arizona (Farley and Dilcher 1986). The specimens used in this study were collected in Ellsworth County, Kansas, and are preserved in ferruginous fine-grained sandstone that represents seasonally water-logged (YPM 26713, nodule) and well-drained (YPM 25365, massive sandstone) levee deposits in a coastal fluvial system (Retallack and Dilcher 2012). Core samples indicate that (1) leaf-bearing nodules, like that of YPM 26713, had an original siderite matrix that has been recently weathered to hematite, and (2) the ferruginous, iron oxide-rich composition of the massive sandstone is original and not the result of oxidative weathering (Retallack and Dilcher 2012).

Hell Creek Flora (Hell Creek Formation, North Dakota).— Specimen YPM 8384 is from the Maastrichtian (ca. 68–65.5 Ma) Hell Creek Formation, collected 75 m below the K–Pg boundary in fluvial deposits in the Williston Basin near Marmarth, North Dakota (Johnson 2002). The leaves from this locality are preserved as impressions in a fine-grained, silt and clay-rich, organic-poor sandstone deposited at the top of point bars (channel lag deposits) in a meandering fluvial system (Johnson 2002).

Fort Union Flora (Fort Union Formation, North Dakota).— Specimen 8366 is from the early Paleocene (ca. 65–63.1 Ma; Peppe et al. 2009) Ludlow Member of the Fort Union Formation, collected ~ 40 m above the K–Pg boundary in the Williston Basin near Marmarth, North Dakota. The leaves are preserved as black compressions in a gray, organic-rich, laminated mudstone deposited in a floodplain pond (Johnson 2002).

Republic Flora (Klondike Mountain Formation, Washington).— Specimen 5995 is from the early Eocene (ca. 49.4 Ma, Moss et al. 2005) 'Republic Flora' of the Tom Thumb Tuff Member of the Klondike Mountain Formation near Republic, Washington (Burnham 1996). Leaves are preserved as impressions in thin diatomaceous laminae within a massive, organic-poor shale rich in volcanic debris that was deposited in a large, deep graben lake (Burnham 1996; Moss et al. 2005).

Florissant Flora (Florissant Formation, Colorado).—Specimen 23724 is from the Oligocene (ca. 35 Ma; Harding and Chant 2000) Florissant Formation. Leaves are preserved as impressions in thin diatomaceous laminae interbedded with clay-rich layers in a finely laminated shale, deposited in a large, deep lake (Harding and Chant 2000; O'Brien et al. 2008).

As the leaves studied in the Dakota Sandstone, Republic, and Florissant floras are not exposed on bedding planes but only as cross-sections perpendicular to the leaf planes, taxonomic assignments are not known. The fragment of YPM 8366 from the Fort Union Formation used for surface analysis is a portion of a dicotyledonous angiosperm, but no more precise classification is available.

Unpolished thin sections were made from fossil-bearing samples cut at least 10 mm from any exposed surface to minimize the effects of surface weathering. Thin sections were made normal to the plane of the leaf in order to facilitate a spatially accurate analysis of the adjacent sediment (Cai et al. 2012). Leaves in the thin sections were visible to the naked eye as thin, dark-toned layers distinct from the surrounding matrix. We were obliged to use unpolished thin sections for all samples because the specimens from Hell Creek and Fort Union proved too friable to survive the polishing procedure, while others were too rich in smectite, which interacted disruptively with epoxy. The use of unpolished sections also avoids contamination with aluminum from the grinding powder.

Modern Biofilms

Six oak leaves (*Quercus alba*) were collected from a single living tree branch on the grounds of the Yale Peabody Museum (New Haven,

Connecticut) and immediately placed in glass vessels which had previously been filled with distilled water (95% by volume) and freshwater mud slurry (5%) from a natural pond (Mill River, Hamden, Connecticut). The slurry was intended to supply both ions and microorganisms. A 0.5 mm sieve was used to remove macroinvertebrates; the resulting mud was composed of fine sand, silt, and small fragments of organic matter. The leaves were not cleaned prior to the experiments, allowing their endogenous and attached microflora to form biofilms and contribute to leaf decomposition. Two leaves were added per container, as replicates. The containers were sealed to minimize evaporation.

The elemental composition of the minerals on the surface of the biofilm in direct contact with the leaves was analyzed after 20, 45, and 100 days of decomposition. Sections approximately 3 mm × 3 mm were sampled from experimentally decayed leaves using a stainless steel scalpel. Sections were mounted on aluminum stubs, where they rapidly dried. Samples were analyzed on the same day as preparation.

Microscopy and Spectroscopy

All fossil and modern (experimental) samples were examined using an FEI/Philips XL-30 field emission environmental scanning electron microscope (FE-SEM) equipped with an EDAX Energy Dispersive X-ray Spectrometer (EDS). All EDS analyses were performed under the same operating conditions: accelerating voltage = 10 kV; working distance = 10 mm; point collection time = 100 seconds. Because SEM-EDS is sensitive to the topography of unpolished thin sections, the measured elemental compositions are qualitatively rather than quantitatively informative. At least 30 point spectra were taken for each of the fossil leaf thin sections, including five points from the leaf tissue, twenty from fine-grained material along the leaf-sediment interface, and five from the matrix. No coating was applied to the thin sections.

Fossil and modern biofilms were identified by comparing the morphology of observed structures and textures with published descriptions (McLean et al. 1999; Westall et al. 2000; Pacton et al. 2007; O'Brien et al. 2008). Multiple points were analyzed using EDS, both (1) on biofilms in direct contact with the modern leaves for each of the 20, 45, and 100-day samples, and (2) on leaf-surface textures observed on the plane of a fossil leaf fragment from the Fort Union Formation in the Bighorn Basin (YPM 8366).

RESULTS

Fossil Leaf Thin Section Analysis

Using backscattered electron imaging on the SEM, leaf tissue was identifiable in all samples as dark linear features of varying thickness, cohesiveness, and texture, revealed by EDS to be richer in carbon than the surrounding material (while clearly distinct both texturally and spectrally from the void-filling epoxy). This may indicate that fossil leaves previously considered to be entirely inorganic impressions in fact retain residual amounts of carbonaceous material. The leaf layers were encased by thin (0.5–2 μm) coatings of minerals that were finer-grained (< 100 nm) than the clastic matrix (which did not show such coatings). Although platy crystals could be resolved in some instances, these coatings were more usually smooth and amorphous. The EDS analyses demonstrated that these boundary minerals were rich in aluminum and silicon (representative spectra shown in Figs. 2–7); we interpret them as poorly ordered nanocrystalline clay minerals (crystallinity was too low for XRD analysis). The presence of these clays may explain the survival of organic matter as a consequence of adsorptive stabilization (e.g., Hedges and Keil 1995). The composition of these clays for each locality is described below and summarized in Table 1. No textures indicative of pyrite framboids or euhedral crystals were observed along the leaf-sediment interface.

Dakota Sandstone Flora.—Only the Dakota Sandstone specimens had a host lithology dominated by sand-sized grains. The elemental composition of the fine-grained fraction of the host matrix in both Dakota Sandstone specimens (YPM 26713, YPM 25365) is predominantly iron-oxide, with minor amounts of Al and Si (Figs. 2C, 2K, 3C, 3J). Backscatter electron imaging and EDS revealed poorly preserved and discontinuous carbonaceous remains associated with void spaces, consistent with the preservation of Dakota Sandstone leaves both in nodules and sandstones as organic-poor adpressions (e.g., Retallack and Dilcher 2012) (Figs. 2, 3).

Clay-sized material along the leaf-interface boundary in both samples was rich in aluminum and silicon, sharply contrasting with the matrix, which was dominated by iron (Figs. 2, 3J) The clay-sized boundary material may reflect an iron-rich aluminosilicate composition or the co-occurrence of iron oxides and aluminosilicates. Four of the five points analyzed along the leaf-sediment interface in both samples contained iron in varying amounts; clays from YPM 26713 (nodule) contain less iron than those in YPM 25365 (sandstone), which were generally iron-rich. The composition of the clays differed more strongly in their trace metal content. The clays in YPM 26713 contained a small amount of additional metal cations in every sample (Na, Mg, and Ca). Two of the boundary points in YPM 25365 contained K, and in one of those two points, Na.

Hell Creek Flora.—The host lithology of YPM 8384 (points 1 and 8 in Fig. 4B) is a sandy siltstone comprised predominantly of O, Al, and Si with minor amounts of metal cations (Ca, Fe, Na, Mg) (Fig. 4C, 4J). The leaf is carbon-rich, but appears to be discontinuous and contains some Al and Si (Fig. 4B, 4D). The cation content of the leaf-sediment interface clays varied and included Ca (point 3), Mg (points 3–5), and K (point 4), and Fe (points 3, 6, 7).

Fort Union Flora.—The host rock matrix of YPM 8366 is composed of only O, Al, and Si (Fig. 5C, 5J). The leaf is preserved as a sediment-filled compression fossil, and the top and bottom cuticles are visible (Fig. 5A); the veins show minimal compression and were unfilled as evidenced by the epoxy in the center which was introduced during preparation of the thin section. Both surfaces of the leaf are preserved as continuous carbon layers, but the internal anatomy of the leaf is not preserved; instead, clay-sized sediment fills the cavity of the leaf. A portion of the ~ 20 μm thick upper cuticle is shown in Figure 5B. The boundary clays contained Mg and other trace metals in varying abundance. Calcium and potassium were found together in three points (points 3, 5, 7; Fig. 5E, 5G, 5I), while two points contained either only Ca (point 6; Fig. 5H) or K (point 4; Fig. 5F). Sodium was found in three points (points 3, 4, 6; Fig. 5E, 5F, 5H). Iron was identified in only one point in the leaf-sediment interface clays (point 3; Fig. 5E).

Republic Flora.—The host matrix of YPM 5595 (points 1, 8; Fig. 6B) is composed of aluminosilicate silts. The leaf is preserved as a semi-continuous carbon rich layer (Fig. 6B, 6D). The boundary clays contain small amounts of Na in combination with various amounts of other cations (Mg, C, and K) and anions (Cl). Iron was not identified in any of the spectra in YPM 5595.

Florissant Flora.—The host matrix of YPM 23724 is a mixture of silt and clay sediments and diatom fragments, with a consistent pure aluminosilicate composition throughout (Fig. 7). The fossil leaf is preserved as a thin, continuous carbonaceous layer. The clays along the leaf-sediment interface are more aluminum-rich than the matrix (points 2, 4, 5, 7; Fig. 7D, 7F, 7G, 7I). Magnesium was identified in three of the four points (points 4, 5, 7), while Ca and Na were present in the other (point 2). Iron was not identified in any of the points analyzed in YPM 23724.

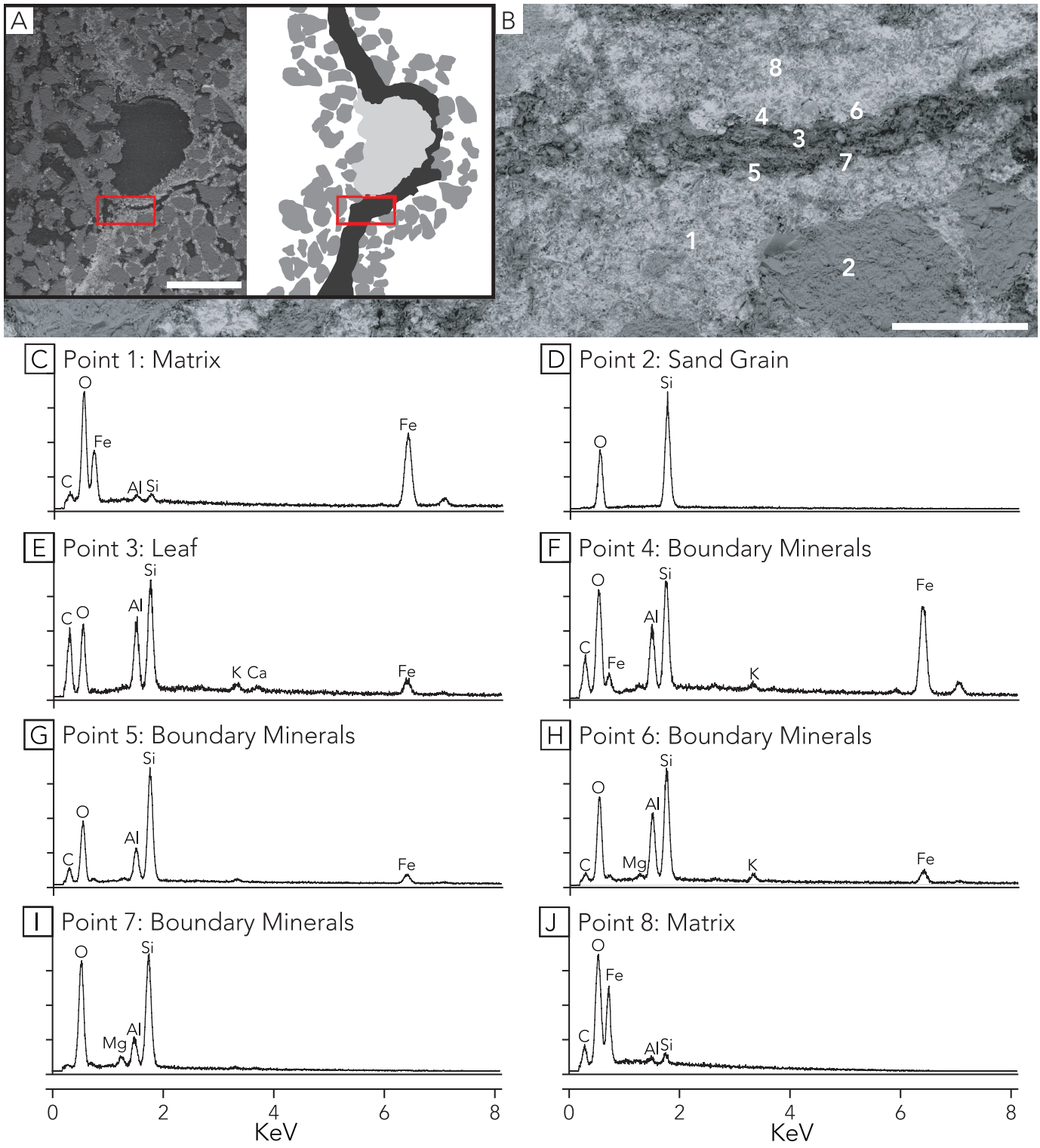

FIG. 2.—SEM images and representative EDS Point Spectra of a thin section through a fossil leaf in a Dakota Sandstone concretion, YPM 26713. **A**) Backscatter electron (BSE) image (left) and cartoon showing a cross section of the leaf (right). The dark central area in the BSE image (light gray in cartoon) is an epoxy filled void space of where a vein was once present. The light gray layer in the BSE image (black in cartoon) is the fine-grained material that preserves the leaf. Sand grains are dark gray in both the BSE image and cartoon. Red boxes show the region examined in B. **B**) BSE image of a portion of the leaf examined using EDS. The dark linear material in the center of B is interpreted to be poorly preserved organic material. Numbers correspond to the locations of the EDS spectra shown in C–J. **C**–**J**) EDS spectra of the matrix surrounding the leaf tissue (C, J), a sand grain (D), the dark leaf tissue (E), and fine-grained minerals along the leaf-matrix boundary (F–I). Scale bars: A = 500 μm; B = 100 μm. Y-axes on EDS spectra indicate relative intensity.

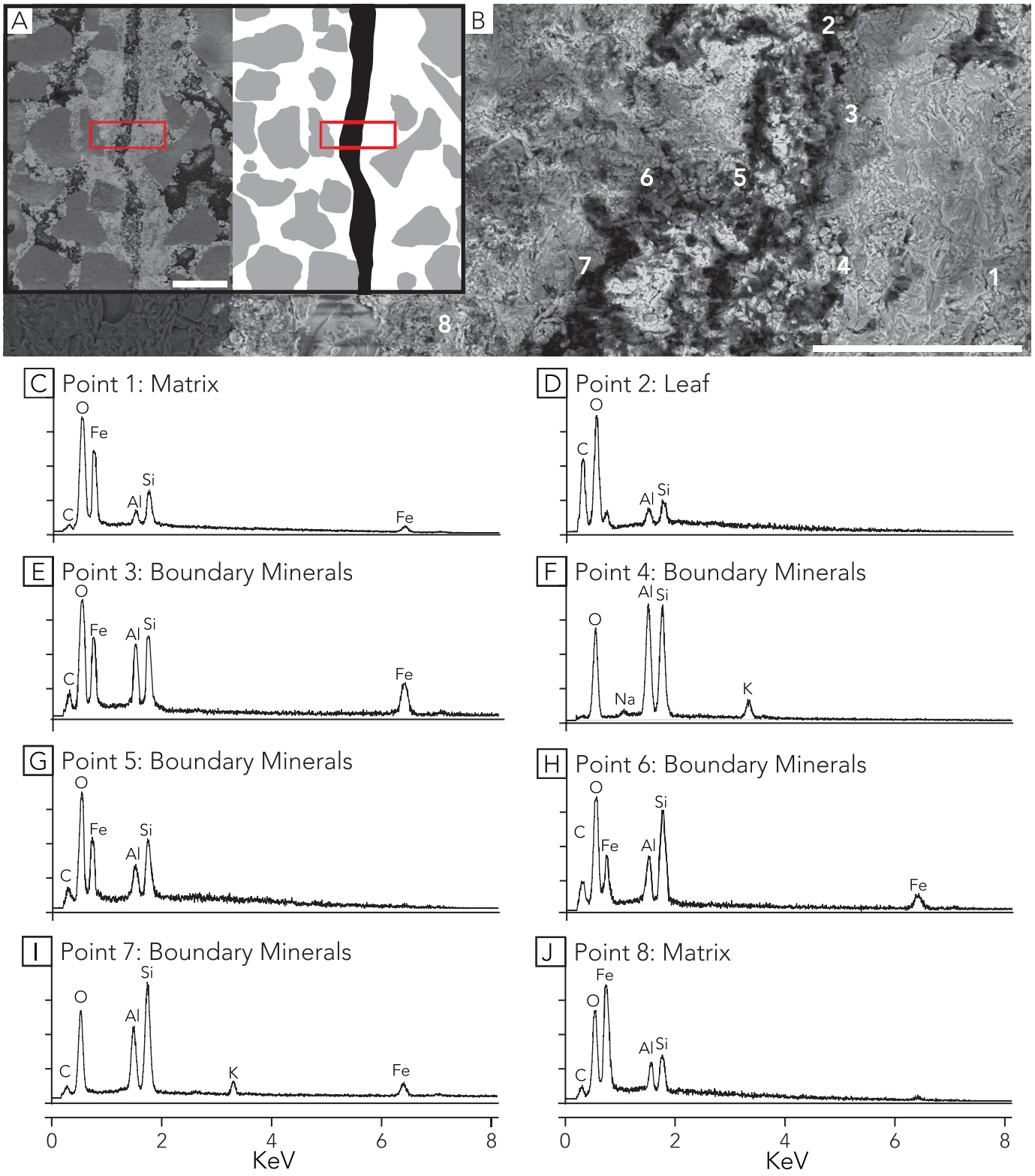

FIG. 3.—SEM images and representative EDS Point Spectra of a thin section through a fossil leaf in the massive sandstone unit of the Dakota Sandstone, YPM 25365. **A**) BSE image (left) and cartoon (right) showing the cross section of the leaf. The dark linear feature running vertically in the BSE image (black portion of cartoon) is the remains of the fossil leaf, which is a void lined by organic-rich material, light gray (white in cartoon) is the iron-oxide matrix, and sand grains are dark gray in both the BSE image and cartoon. Red boxes show area examined in B. B) BSE image of a portion of the leaf examined using EDS. The dark feature in the center of B is interpreted to be material with some organic matter lining a void (bright white). Numbers correspond to the locations of the EDS spectra shown in C-J. C-J) EDS spectra of the matrix surrounding the leaf tissue (C, J), the leaf tissue (D), and fine-grained minerals along the leaf-matrix boundary (E-I). Scale bars: A = 500 μm; B = 50 μm. Y-axes on EDS spectra indicate relative intensity.

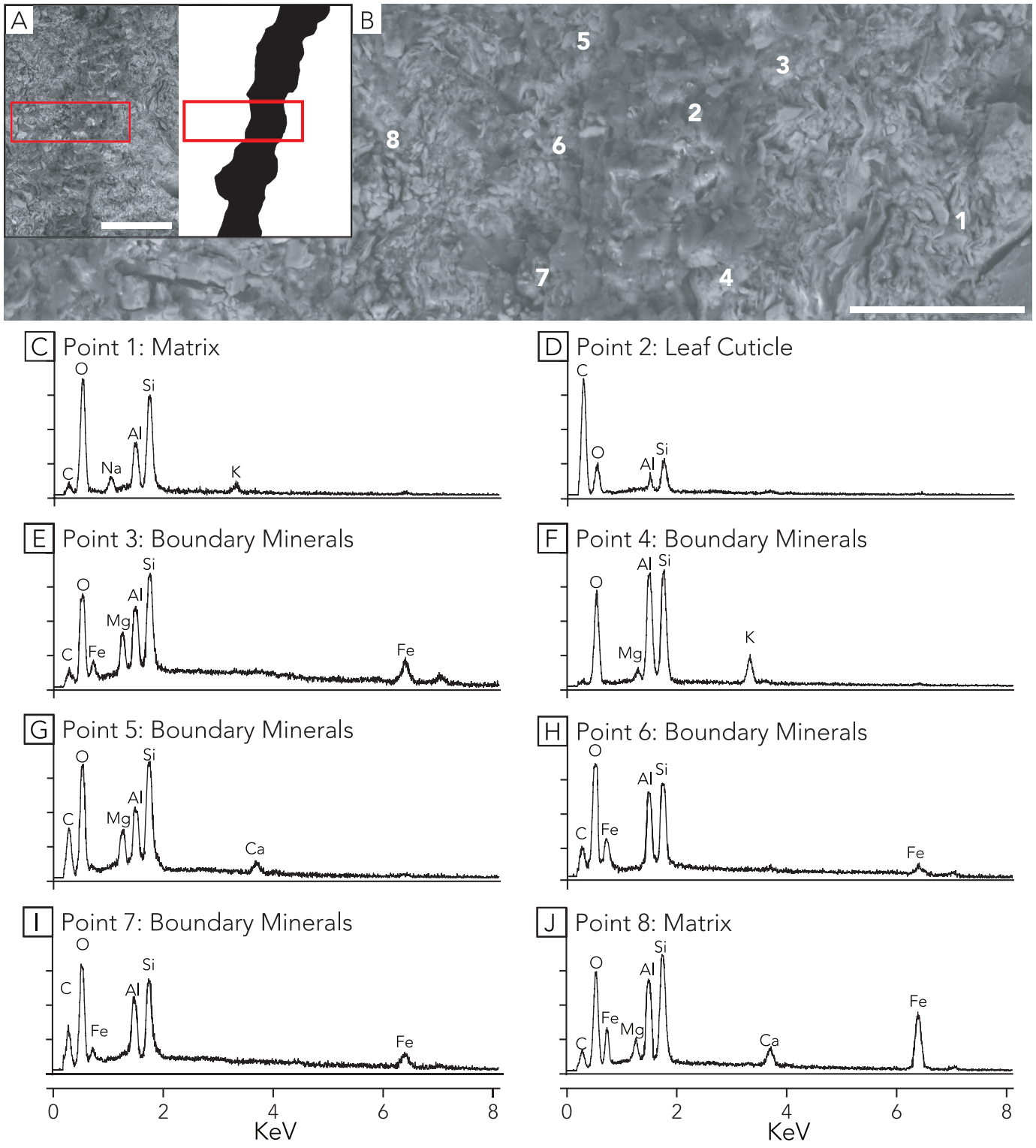

FIG. 4.—SEM images and representative EDS Point Spectra of a thin section through a fossil leaf from the Hell Creek Formation, YPM 8384. **A**) BSE image (left) and cartoon (right) showing the cross section of the leaf. The dark linear feature running vertically in the BSE image (black portion of cartoon) is the remains of the fossil leaf encased in a clay-rich siltstone (white portion of cartoon). Red boxes show area examined in B. **B**) BSE image of a portion of the leaf examined using EDS. The dark, smooth feature in the center of B is interpreted to be material with some organic matter lining a void (bright white). Numbers correspond to the locations of the EDS spectra shown in C–J. **C**–**J**) EDS spectra of the matrix surrounding the leaf tissue (C, J), the leaf tissue (D), and fine-grained minerals along the leaf-matrix boundary (E–I). Scale bars: A = 100 μm; B = 30 μm. Y-axes on EDS spectra indicate relative intensity.

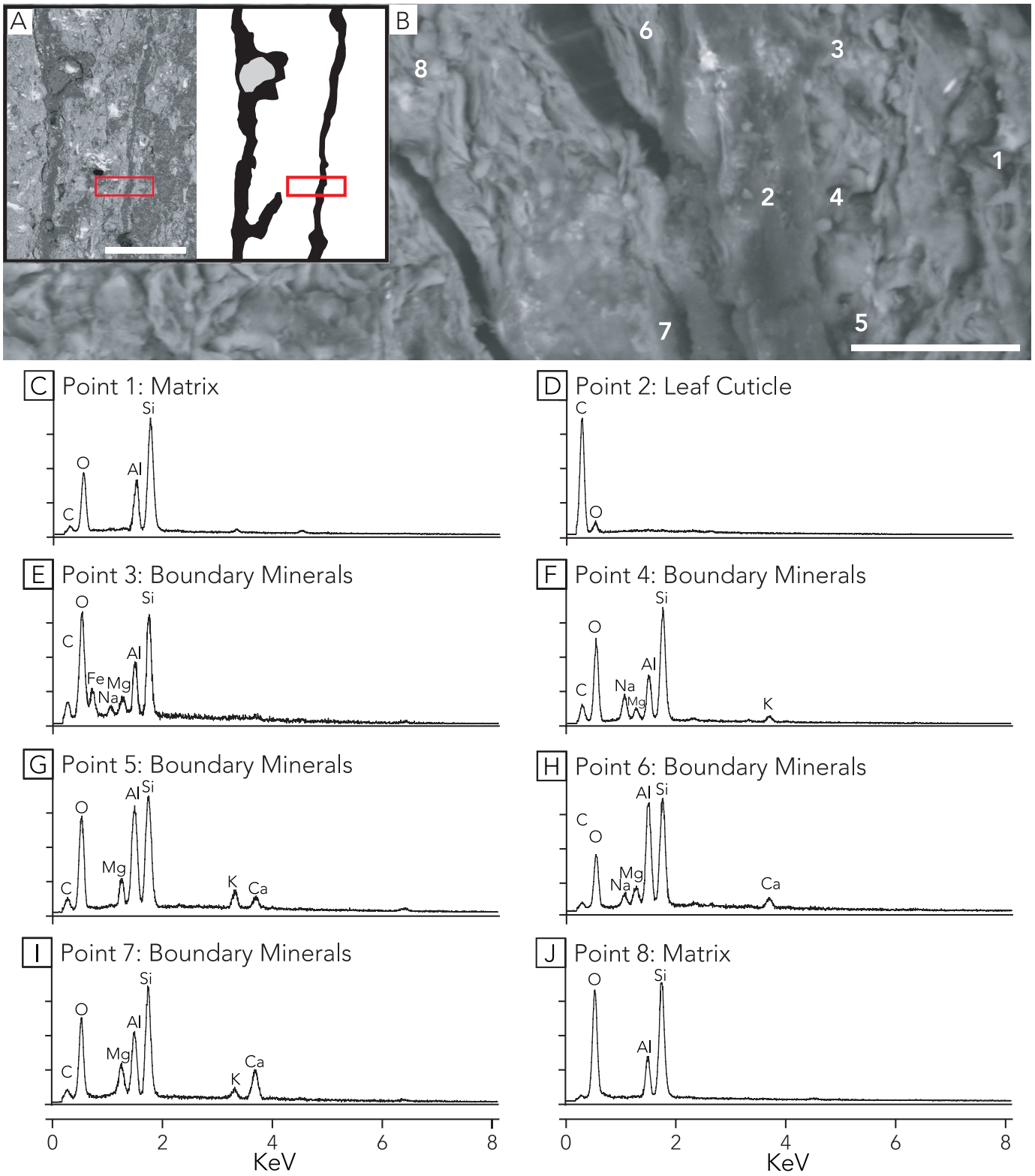

FIG. 5.—SEM images and representative EDS Point Spectra of a thin section through a fossil leaf from the Fort Union Formation, YPM 8336. **A**) BSE image (left) and cartoon (right) showing the cross section of the leaf. The dark linear features running vertically in the BSE image (black portion of cartoon) are the remains of the fossil leaf preserved as a sediment-filled compression encased in a clay-rich siltstone (white portion of cartoon). Vein is filled with epoxy (gray area in cartoon). Red boxes show area examined in B. **B**) BSE image of a portion of the leaf examined using EDS. The dark, smooth material in the center of B is the fossil leaf. Numbers correspond to the locations of the EDS spectra shown in C–J. **C**–**J**) EDS spectra of the matrix surrounding the leaf tissue (C, J), the leaf tissue (D), and fine-grained minerals along the leaf-matrix boundary (E–I). Scale bars: A = 500 μm; B = 50 μm. Y-axes on EDS spectra indicate relative intensity.

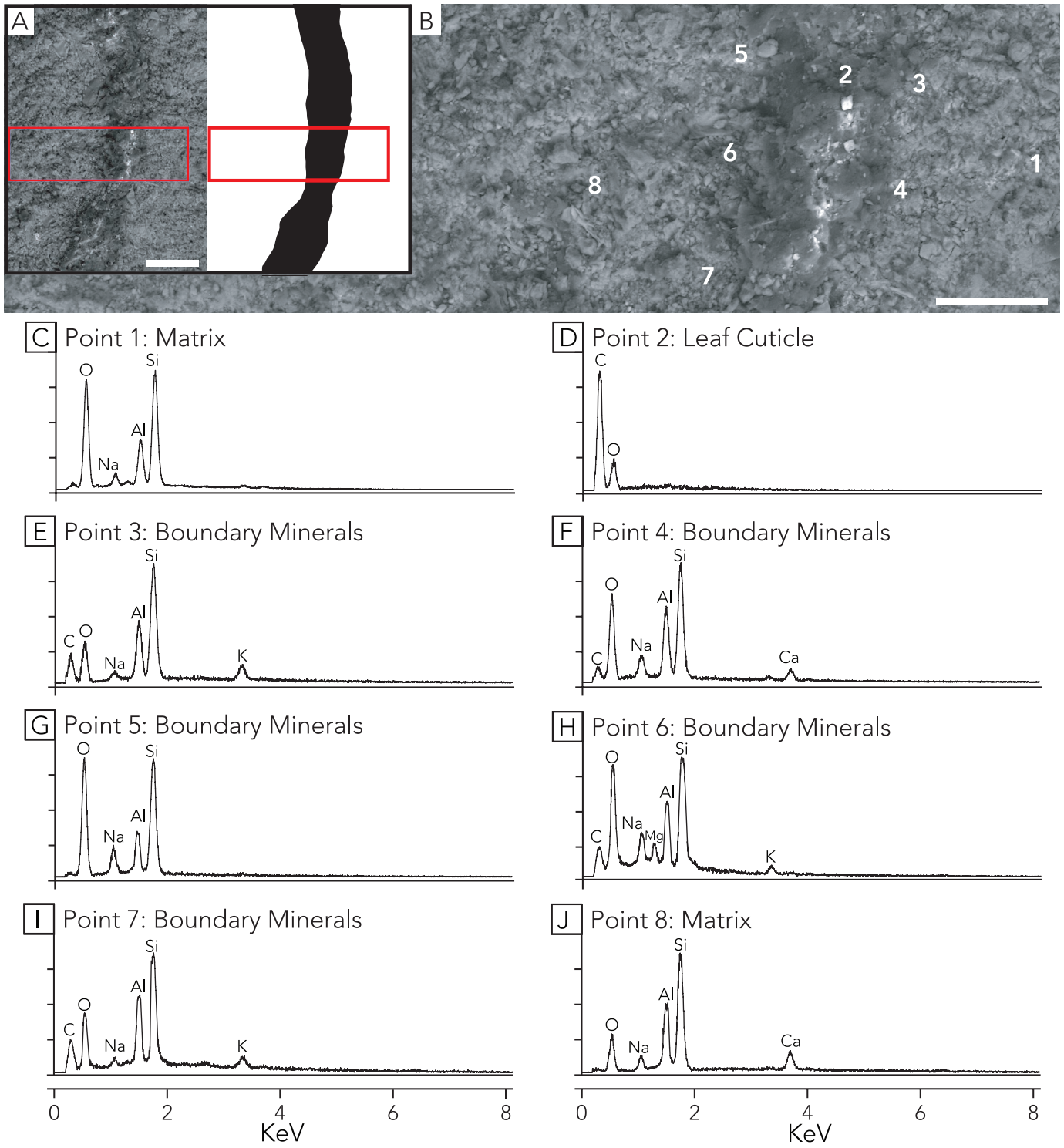

FIG. 6.—SEM images and representative EDS Point Spectra of a thin section through a fossil leaf from the Republic Flora, YPM 5995. **A**) BSE image (left) and cartoon (right) showing the cross section of the leaf. The dark linear features running vertically in the BSE image (black portion of cartoon) are the remains of the fossil leaf preserved as an oxidized compression encased in a clay-rich siltstone (white portion of cartoon). Red boxes show area examined in B. **B**) BSE image of a portion of the leaf examined using EDS. The dark, smooth material in the center of B is the fossil leaf. Numbers correspond to the locations of the EDS spectra shown in C–J. **C**–**J**) EDS spectra of the matrix surrounding the leaf tissue (C, J), the leaf tissue (D), and fine-grained minerals along the leaf-matrix boundary (E–I). Scale bars: A = 50 μm; B = 25 μm. Y-axes on EDS spectra indicate relative intensity.

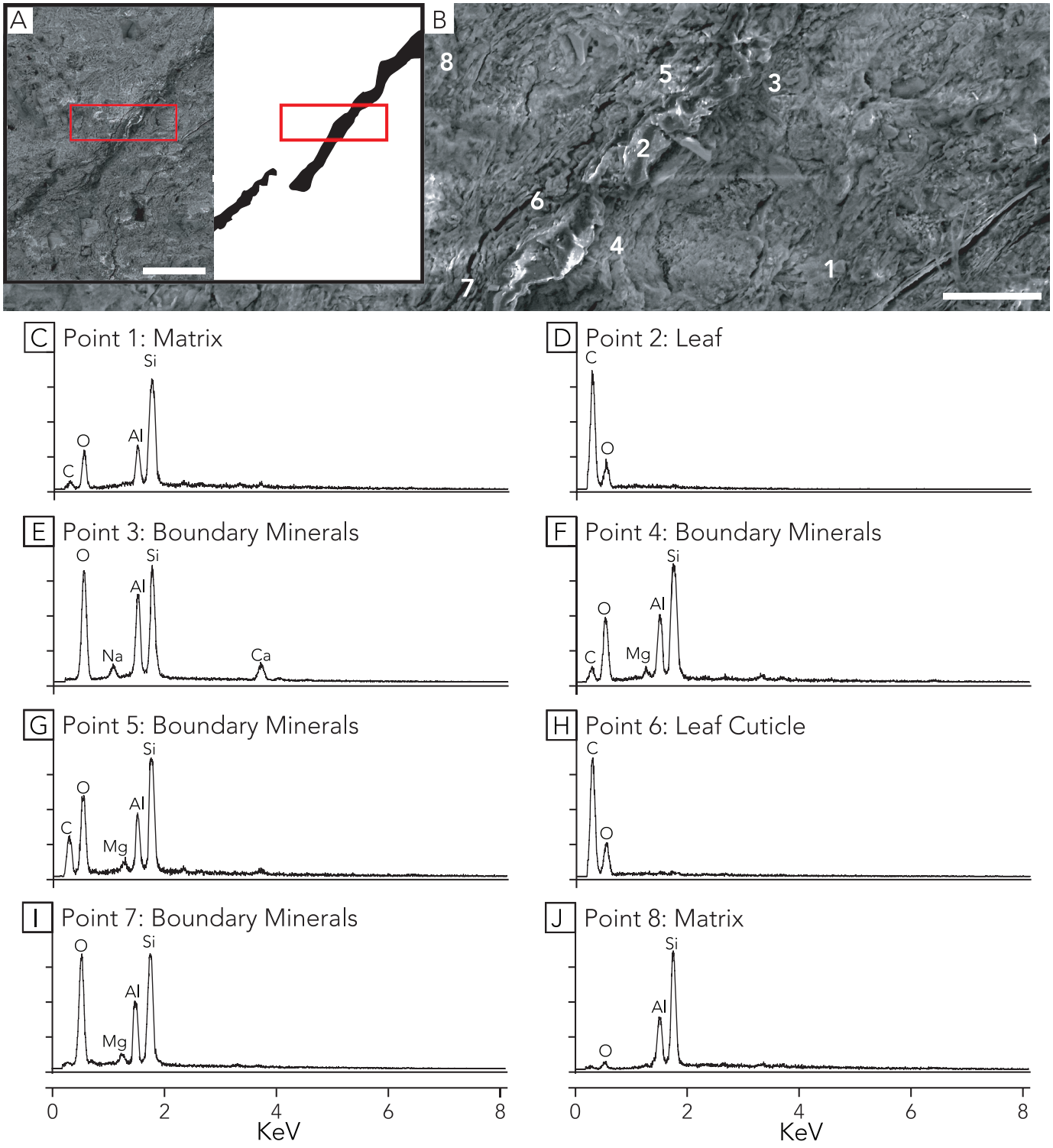

FIG. 7.—SEM images and representative EDS Point Spectra of a thin section through a fossil leaf from the Florissant, YPM 23724. **A**) BSE image (left) and cartoon (right) showing the cross section of the leaf. The dark linear features running vertically in the BSE image (black portion of cartoon) are the remains of the fossil leaf preserved as an oxidized compression encased in a clay-rich siltstone (white portion of cartoon). Red boxes show area examined in B. **B**) BSE image of a portion of the leaf examined using EDS. The dark, smooth material in the center of B is the fossil leaf. Numbers correspond to the locations of the EDS spectra shown in C–J. **C**–**J**) EDS spectra of the matrix surrounding the leaf tissue (C, J), the leaf tissue (D), and fine-grained minerals along the leaf-matrix boundary (E–I). Scale bars: A = 50 μm; B = 25 μm. Y-axes on EDS spectra indicate relative intensity.

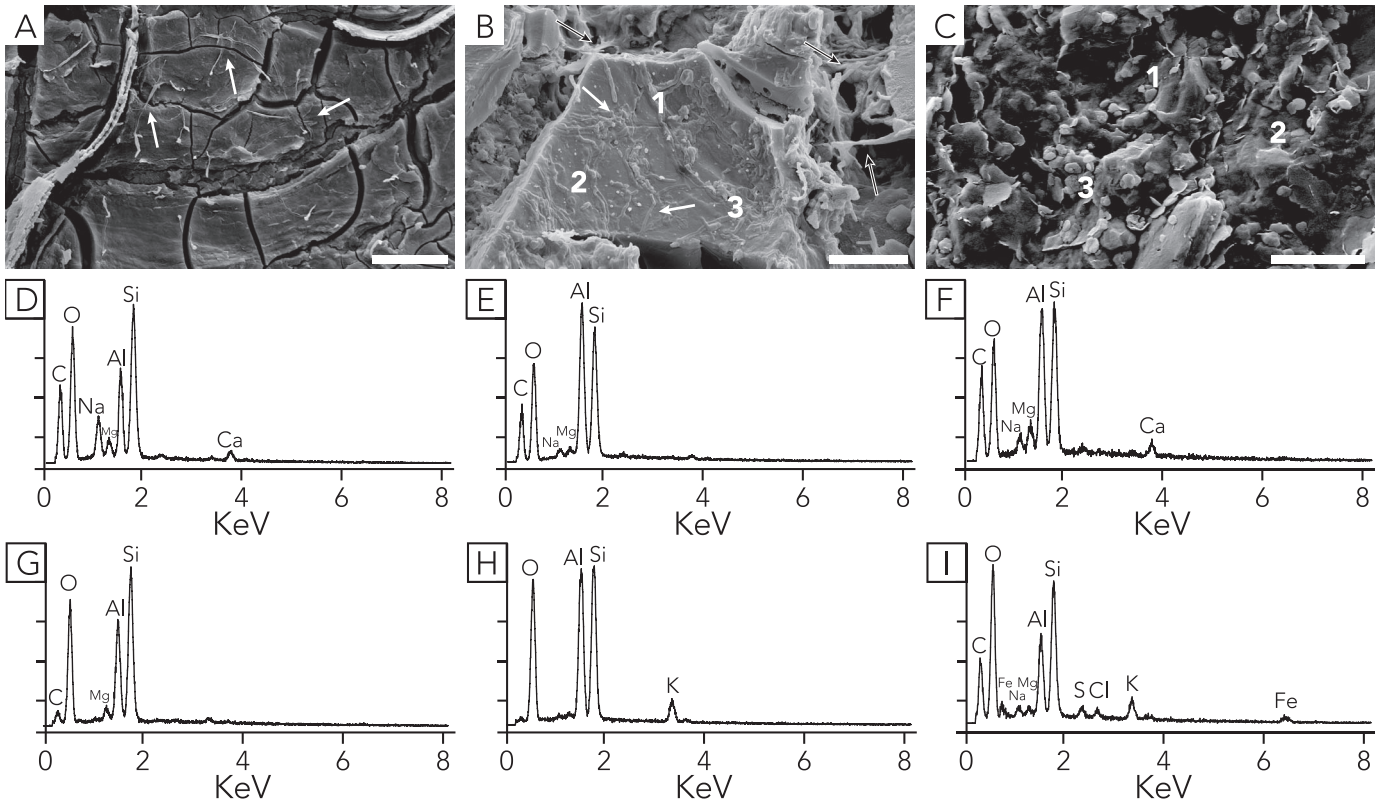

FIG. 8.—SEM images and EDS point spectra of biofilms and associated clays preserved on a leaf compression from the Fort Union Formation. **A**) SEM image of a fossil leaf surface preserved under a biofilm formed from overlapping filaments (white arrows). **B**) SEM image of a leaf surface with filaments on the surface (white arrows), and amorphous and alveolar-type biofilms (black arrows). Numbers 1, 2, and 3 correspond to EDS point spectra D, E, and F respectively. **C**) SEM image of platy clay sized particles encased in an amorphous biofilm veil. Numbers 1, 2, and 3 correspond to EDS points spectra shown in G, H, and I respectively. **D**–**I**) EDS point spectra showing the composition of biofilms. Scale bars: A = 20 μm; B = 10 μm; C = 5 μm. All spectra are indicative of aluminosilicates. Y-axes on EDS spectra indicate relative intensity.

Fossil Biofilms

Strands, filaments and amorphous materials cover much of the surface of the fossil leaf fragment from the Fort Union Formation (Fig. 8A–8C). These include common, thin (< 1 μm) filaments of near-constant diameter, which vary from flat to semi-cylindrical and criss-cross over the leaf (Fig. 8A, 8B) (cf. Pacton et al. 2007, fig. 7). Less commonly, amorphous organic matter forms veils and alveolar networks (Fig 8B) and surrounds particles of clay (Fig. 8C). Diatoms were observed in thin section in close association with leaves of the Hell Creek and Florissant floras (diatomaceous biofilms have previously been reported in association with the latter; O'Brien et al. 2008).

Elemental analyses were conducted on two areas of the Fort Union Formation leaf where exhibiting different surficial morphologies. The first set of elemental analyses was conducted in a section of the leaf with small (< 0.5 μm) mineral grains both on the surface and embedded within an amorphous, gel-like, massive structure which we interpret as a fossil biofilm (Fig. 8B). Most grains are roughly hexagonal and platy (e.g., points 1 and 2, Fig 8B); rare aggregations of rounded granules are present (point 3). The platy minerals had similar compositions almost entirely O, Al, and Si, with small amounts of either Mg (point 1) or K (point 2). The granular minerals had a much more diverse composition, with several cations (Fe, Na, Mg, and K) and anions (S, Cl). The second set of analyses was conducted on an area of leaf cuticle densely covered in filaments which we interpret as fossil EPS (Fig. 8B, 8D–8F). The smooth appearance of the inferred biofilm filaments suggests that the authigenic precipitates are nanoparticles (3–5 nm) (Glasauer 2011) which are not visible at the resolution capabilities of the available SEM. The elemental composition of the three points varied slightly. All EDS point spectra were dominated by O, Al, and Si, and had a moderate C peak and small Na and Mg peaks (Fig. 8G–8I). Calcium was identified as a minor component in two points (Fig. 8D, 8F) and is absent from the third, which was the only point containing Fe and K, and in lesser amounts, S and Cl (Fig. 8E).

Modern Biofilms

Within 20 days, the oak leaves had developed a diatom-dominated biofilm (Fig. 9). Portions of the leaf were obscured by a thick layer of diatoms (Fig. 9A), while others revealed textures characteristic of EPS from microbial biofilms (Fig. 9B) (Pacton et al. 2007). Elemental analyses were conducted on points on these biofilms in direct contact with the leaf surface; a representative EDS spectrum is presented in Figure 9C. Oxygen, Si, and Fe are the major components identified in the biofilm, with moderate amounts of C, Al, and Ca and minor amounts of S and K. The vessels were sealed and evaporation was not observed, and could not have caused the observed ion enrichments.

The elemental compositions of the biofilm in leaves sampled after 45 days and 100 days in the experimental vessels were significantly different compared to those after 20 days. Diatoms were generally less dense at the 45-day sampling point, but EPS was found to cover much of the leaf and was often associated with small patches of sediment and diatoms (Fig. 9D, 9E); this change was accompanied by a loss of Fe and S from the EDS spectra. After 100 days, much of the surface of the sampled leaf was

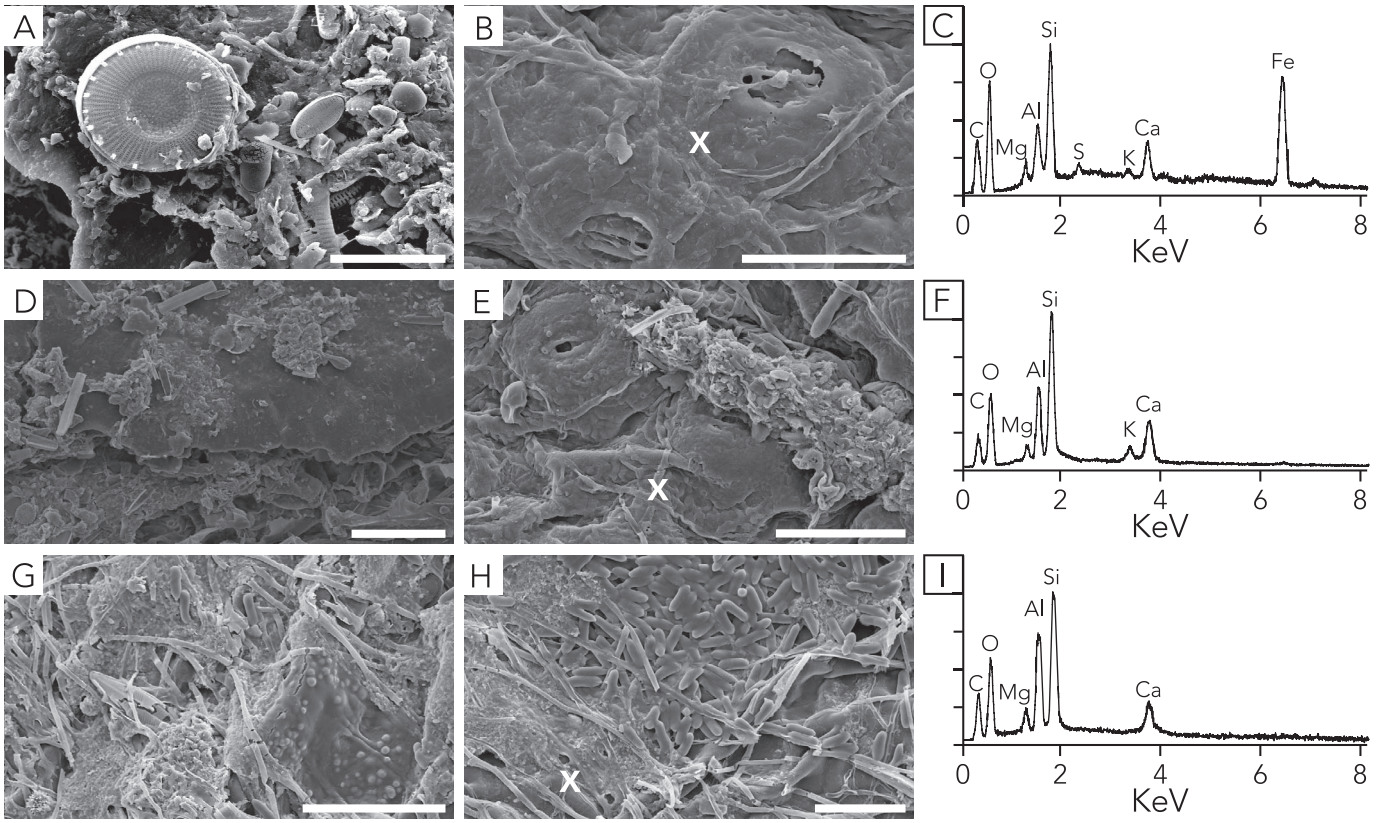

FIG. 9.—SEM images and representative EDS point spectra of biofilms and associated clays on the surface of a modern oak leaf decaying in fresh water. The 'X' in B, E, and H mark the location of the point spectra presented in C, F, and I. **A**–**C**) After 20 days of decay. **D**–**F**) After 45 days of decay. **G**–**I**) After 100 days of decay. Each SEM image was taken from a different individual leaf. See text for explanation and interpretation. Scale bars: A, H = 10 μm; B, E, G = 20 μm; D = 50 μm. Y-axes on EDS spectra indicate relative intensity.

covered by a combination of EPS, fungal hyphae, and bacteria of filamentous, coccoidal, and bacillary morphology (Fig. 9G, 9H). Despite the changes in microbial community layers on the surface of the leaves, the elemental composition of the biofilm in contact with leaf surfaces remained essentially the same as the 45-day sampling point. The primary difference between the spectra is an increase in Al and a loss of K after 100 days (Fig. 9I).

DISCUSSION

Our results are consistent with previous studies demonstrating the importance of microbial biofilms in leaf preservation (e.g., Dunn et al. 1997; Harding and Chant 2000; Allison et al. 2008), but show a heretofore unrecognized, widespread association of clays with LAFs. Although few in number, the leaf fossils included in this study represent diverse depositional environments, ages, lithologies, and modes of adpression preservation, and all of them are encased in fine-grained aluminosilicates distinct in appearance and composition from the surrounding matrix. We included one leaf interpreted as an organic compression fossil (Fort Union), and our analyses show that clays are also associated with this mode of leaf adpression. These data support our hypothesis of a widespread clay-based mode of fossil leaf preservation, even in the Dakota Sandstone studied by Spicer (1977), where leaf boundaries are enriched in clay and not iron oxide compared to the matrix cements. In other flora no spectra taken along the leaf-sediment interface indicated the presence of iron, and most lacked iron altogether.

The presence of distinct clays associated with fossil leaf impressions—despite substantial differences in their origin and placement along the adpression continuum (more-to-less organic retention)—suggests that a shared taphonomic process is commonly involved in leaf preservation (Cai et al. 2012; Meyer et al. 2012). Before a taphonomic model of leaf preservation can be developed, however, the origin of these clays must be established. In the following sections, we discuss the role of clays in the preservation of other soft-bodied fossils, the nature of the clays in association with the fossil leaves included in this study, and a new taphonomic hypothesis to explain the variation observed in LAFs more widely.

Clay Preservation in Soft-Bodied Fossils

Previous documentation of aluminosilicates involved with the preservation of soft-bodied compression fossils is largely confined to studies of Mesoproterozic (e.g., Wacey et al. 2014), Ediacaran (e.g., Laflamme et al. 2011; Meyer et al. 2012), and early Paleozoic marine rocks (e.g., Gabbott et al. 2001), with a single report of aluminosilicification in an early Cretaceous lacustrine deposit (Pan et al. 2014).The origin of this clay-fossil relationship and the role of aluminosilicates in fossilization have been at the center of recent debates, particularly in relation to Burgess Shale-type fossils preserved as carbonaceous compressions enveloped (or 'templated') by a thin aluminosilicate veneer (Butterfield et al. 2007; Page et al. 2008; Anderson et al. 2011; Cai et al. 2012; Meyer et al. 2012). The recognition of clay-templating as a preservational process has been controversial due, in large part, to the burial history of many of the host rocks, which makes it difficult to distinguish clays precipitated or attached to fossils during early diagenesis from *de novo* artifacts of metamorphism or late diagenesis (Butterfield et al. 2007; Meyer et al. 2012; Forchielli et al. 2014).

In some fossil faunas, identical clays occur on the fossil and in the matrix, which hinders our ability to discern the fossil-clay relationship (Gaines et al. 2008; Pan et al. 2014). When present, compositionally distinct clays are associated almost exclusively with only recalcitrant surface tissues in two-dimensional compression fossils, indicating they may have adsorbed to tissues later in diagenesis and did not play a constructive role in fossil preservation (Cai et al. 2012; Pan et al. 2014). However, careful analyses have shown that the clays found in association with some compression fossils most likely represent either in-life clay attachment (e.g., agglutination) or early authigenic clays or clay-precursors precipitated on tissues (Anderson et al. 2011; Meyer et al. 2012). The fine-grained material found on the surface of Ediacaran impression fossils in sandstones has also been argued to result from microbially mediated precipitation of pyrite and aluminosilicates (e.g., Laflamme et al. 2011). Clay-templated carbonaceous compressions and clay-enhanced Ediacaran-style impressions may share the following alteration-resistant traits useful for identifying authigenic clays in other fossils: (1) finer grain size than the surrounding matrix; (2) an aluminum-enriched composition compared to that of the surrounding matrix; and (3) restriction of the clay to the area immediately surrounding the fossil (Laflamme et al. 2011; Meyer et al. 2012).

Origin of Clay in Fossil Leaves

In contrast to many Precambrian and Paleozoic fossils, the fossil leaves included in this study are preserved in rocks deposited in freshwater settings that have been not exposed to elevated temperatures or pressures by deep burial (all $<$ 1 km maximum burial depth; $<$ 25° C; $<$ 25 bar) or hydrothermal fluids (see Meyer 2003; Retallack and Dilcher 2012), excluding the possibility of a metamorphic origin of the observed clays. The most significant diagenetic process known to have affected some of the localities is recent oxidative weathering (Republic, Leopold et al. 1996; Dakota Sandstone nodules, Retallack and Dilcher 2012; Florissant, McNamara et al. 2012), potentially resulting in several chemical and textural alterations: a reduction in the quality of carbonaceous preservation; the transformation of reduced iron minerals (e.g., pyrite, siderite) to iron oxides; the enrichment of purer aluminosilicates (kaolinite, illite) with iron and magnesium to form smectite or chlorite; and an increase in iron oxide crystallinity (Forchielli et al. 2014; Potter-McIntyre et al. 2014). Although some of these modifications are likely to have affected the fossil leaves—particularly the degradation of leaf organic matter—the preferential precipitation of the cation-rich aluminosilicate layers directly along leaf surfaces is highly unlikely to be the result of these late processes.

The clays observed in association with the fossil leaves must therefore be either the result of authigenic precipitation or early attachment. Several lines of evidence suggest that the clay-leaf association identified in fossil leaves from all five localities is the result of early microbial biofilm-mediated authigenic clay precipitation.

Grain Size and Appearance.—Microbially mediated authigenic clays can be distinguished from detrital grains by their small grain size and poorly ordered structure (Konhauser and Urrutia 1999; Meyer et al. 2012). The minerals we observe along leaf-sediment interfaces are almost all finer-grained than the resolving power of the SEM ($<$ 100 nm), and appear to be either poorly ordered or nanocrystalline under the SEM, consistent with the bacterial authigenic clays observed in experiments by Konhauser and Urrutia (1999). Increased crystallinity of poorly ordered authigenic clays can occur through dehydration over the course of years (Konhauser and Urrutia 1999), but authigenic clays may remain amorphous or poorly ordered after more than a billion years (e.g., Wacey et al. 2014). In the few instances where crystallinity was resolvable, boundary clays exhibited a somewhat platy habit, with the surface of the mineral grains aligned parallel to the leaf (e.g., Fort Union, point 6, Fig. 5; Florissant, points 6 and 7, Fig. 7), consistent with the orientation of bacterial authigenic clay grains with a more crystalline form (Konhauser and Urrutia 1999). By contrast, detrital clays with a platy habit that adsorb onto biofilms tend to attach perpendicularly along their more reactive edges (Konhauser and Urrutia 1999).

Elemental Composition.—Clays precipitated in association with a biofilm are compositionally distinct from minerals formed in the environment outside of the biofilm (Konhauser 1998). Authigenic clays precipitated by biofilms are generally enriched by a variety of metal cations such as Al, Na, K, and Fe (e.g., Souza-Egipsy et al. 2005; Meyer et al. 2012; Bontognali et al. 2014). The results of our study show that the composition of clays along the leaf-sediment interface can vary within micrometers, but that these are more similar to one another and more metal-rich than grains in the surrounding rock, consistent with a microbial authigenic origin. For most of the fossil localities included in this study, the clays along the leaf-sediment interface are iron-poor and aluminum-rich relative to the surrounding grains. Where aluminum does occur in the matrix or cement, it is usually not associated with the calcium or potassium typical of the leaf boundary material, implying a difference between the leaf boundary clay and clay in the surrounding sediment.

Taphonomic experiments presented in this study and by others (e.g., Urrutia and Beveridge 1994) demonstrate that iron-rich aluminosilicates form in a matter of hours in association with microbial biofilms and the decomposition of organic matter in a range of aqueous and sediment conditions. However, depending on the availability of ions, authigenic clays may become less ferruginous, more siliceous, and richer in aluminum and other cations over a matter of days to weeks, as occurred during the decay of oak leaves in this study and in previous experiments (Kawano and Tomita 2001; Michalopoulos and Aller 2004). Iron may be replaced by potassium later in diagenesis as the result of anaerobic iron-reductive microbial degradation of the organic leaf material in the subsurface (Vorhies and Gaines 2009). Thus, an authigenic origin can account for both the iron-enriched and iron-poor boundary clays observed in fossil leaves.

Biofilms.—The rapid formation of a microbial biofilm on oak leaves in our experiments is consistent with previous observations of biofilm growth on leaves in both laboratory decay experiments (Locatelli et al. 2016) and natural settings (e.g., McNamara and Ledge 2004; Wright and Covich 2005). Decaying leaves are an important carbon source and colonizable substrate in freshwater systems, and favor the growth of specific biofilm-forming communities (e.g., Meyer et al. 1998; Das et al. 2007) different from those in the surrounding sediment (Beier et al. 2008). The indigenous microflora attached to living leaves includes biofilm producers (Morris et al. 1997), and additional colonization of leaf surfaces by diatoms, bacteria, and other microbes and the subsequent production of an EPS matrix occurs ubiquitously in terrestrial aquatic and soil environments, regardless of oxygen levels, pH, temperature, and metal content of the water (e.g., Konhauser 1998; Konhauser et al. 1993, 1998). Biofilm formation is essential for the precipitation of clays (and other minerals) onto leaf surfaces. Ions and mineral grains do not generally bind to leaf surfaces in the absence of biofilms because most leaves are waxy and inert (Kok and Van der Velde 1994; Dunn et al. 1997).

The features we observed on the fossil leaf surface from the Fort Union Formation were consistent with the morphology and texture of both modern and fossil biofilms (microbial cells and associated EPS) with and without visible mineral precipitates (e.g., McLean et al. 1999; Westall et al. 2000; Pacton et al. 2007). Direct evidence for the organismal origin (bacteria, diatoms) is mostly lacking, which is common in fossil biofilms (Westall et al. 2000). However, the visible presence of diatoms in close association with leaves in the Hell Creek and Florissant thin sections provides additional support for a biofilm-mediated origin of the observed clays. A role for diatom blooms or mats in the preservation of the Republic

flora and coeval lacustrine Lagerstätten in British Columbia has been inferred previously (Archibald et al. 2011; Mustoe 2005). Moreover, diatomaceous biofilms have previously been reported on Florissant leaves, and may have been involved in the preservation of the Republic flora (Mustoe 2005; O'Brien et al. 2008; Archibald et al. 2011).

The 'Biofilm-Clay Template' Model of Leaf Preservation

In the preceding sections, we have established that (1) the fine-grained minerals directly in contact with the surface of LAFs from multiple fossil floras are aluminosilicates: (2) these clays differ in their elemental composition from the surrounding sediments; and (3) these clays reflect a microbially mediated authigenic origin. Based on our results, we propose a model of leaf fossilization that begins with microbially mediated aluminosilicate precipitation (which we here call the 'Biofilm-Clay Template' model) (Fig. 10), which reflects earlier models of leaf preservation that recognize the importance of early mineralization and microbial biofilms (e.g., Spicer 1977; Dunn et al. 1997). In this model, the formation of a biofilm-clay template does not dictate the final mode of preservation. Rather, a biofilm-clay template is the first step in fossilization and may be followed by additional forms of mineralization, resulting in the diverse forms of leaf adpressions observed in the fossil record (Fig. 10D, 10E).

The process of biofilm-clay template formation begins after a leaf enters either the litter or an aqueous environment. A variety of microbes, including archaea, bacteria, fungi, and diatoms from both the native leaf microflora and the wider depositional setting colonize the leaf surface and interior and excrete various substances (EPS), forming a biofilm (Fig. 10A). The composition of the community that initiates colonization of the leaf is highly contingent and sensitive to the environment; it will depend upon, among many other things, whether the leaf is decaying subaerially in moist soil, or floating, submerged, or buried in oxygenated, dysoxic, or anoxic water or sediments. The process of biofilm-clay template formation requires a moist environment, as both biofilm formation and ion transport require water. Dissolved metals in the form of either free ions or oxides/oxyhydroxides—predominantly aluminum and iron species due to their reactive nature and abundance in most freshwaters and associated sediments and soils (Konhauser et al. 1993; Konhauser and Urrutia 1999)—adsorb to the biofilm (Fig. 10B). These adsorbed metals provide binding sites for silica, and, ion availability permitting, result in the nucleation of nanocrystalline, poorly ordered aluminosilicates and their precursors on the surface and within the biofilm—thus forming the biofilm-clay template (Fig. 10C).

The thickness, microbe-to-clay ratio, density, and exact elemental composition of the biofilm-clay template varies depending on the nature of the biofilm (both its organic composition and microbial community: Michalopoulos and Aller 2004; Pacton et al. 2007), availability of metals, burial rate, sediment permeability, and oxygen concentrations (Konhauser 2011; Mikutta et al. 2011). For example, a biofilm-clay template forming under oxidizing iron-rich, silica depleted tropical soils may be composed of a mixture of aluminosilicates and iron oxides (Locatelli 2013), whereas leaves encased in a diatomaceous biofilm within a lake will have more aluminum, potassium, and silicon (Michalopoulos and Aller 2004; Allison et al. 2008). Microbial decay, particularly via anaerobic iron-reducing respiration, may affect the elemental composition of the clay precipitates, as living cells actively scavenge certain metals (e.g., K, Mg, Na) required for metabolism and remove reactive iron (III) from the available metal pool, resulting in the concentration of aluminum within the EPS matrix of the biofilm (Konhauser et al. 1993).

A biofilm-clay template may promote fossilization in a number of ways, and may enhance leaf preservation differently depending on the depositional setting and exact nature of the biofilm-clay template. The biofilm-clay template may provide physical protection, form a barrier to oxidative reactants, promote the stabilization of the surrounding sediments through continued adsorption and precipitation, and prevent compaction of the decayed leaf during burial (Dunn et al. 1997; Spicer 1977; Salmon et al. 2000; Briggs 2003). A biofilm-clay template may provide biochemical protection by reducing or inhibiting microbial respiration and autolytic enzymes, increasing the short-term recalcitrance of more labile leaf tissues, and enabling kerogen formation (Salmon et al. 2000; Wilson and Butterfield 2014).

The final mode of adpression of a fossil leaf reflects the interaction between the rate of burial, microbial respiration, initial environmental conditions, sediment grain size, and later diagenetic processes (Fig. 10). Although grain size may determine the absolute degree of compaction during early diagenesis (Rex and Chaloner 1983; Rex 1986), the rate of burial has a greater impact on whether a leaf will be preserved as a flat-lying, archetypal adpression (slow burial) or a more three-dimensional leaf mold (rapid or catastrophic burial), given the same leaf structure and composition (Rex and Chaloner 1983).

Flat-lying adpressions are formed in relatively low-energy aqueous conditions, where fine-grained lake sediments (e.g., Fort Union, Republic, Florissant) or coarser fluvial sediments (e.g., Hell Creek, some fossils from the massive Dakota Sandstone) accumulate. Flat-lying adpressions form when leaves sink through the water column, coming to rest on the sediment-water interface (upper leaf Fig. 10A–10C, 10D). The initial formation of the biofilm-clay template can take place in the water column or at the sediment-water interface. As with all forms of soft-tissue preservation, the preservation of leaves under slow burial conditions requires that mineralization outpaces decay. In well oxygenated environments, leaves are degraded rapidly by both biological processes (Webster and Benfield 1986) and chemical oxidation (Mikutta et al. 2011), and the preservation of intact leaves is unlikely. Indeed, the formation of biofilms on leaves in oxic lakes may attract larger invertebrates, resulting in fragmentation (e.g., Webster and Benfield 1986). Dysoxic or anoxic conditions will also allow the development of bacterial biofilms, but largely exclude the obligate aerobic fungi and detritivores (Wright and Covich 2005) and lessen the extent of chemical oxidation. Under these conditions, decay is slowed, as anaerobic bacteria are less efficient at breaking down many of the complex, recalcitrant tissues in leaves (e.g., cutin, lignin; Gallardo and Merino 1993; Wright and Covich 2005).

Even in fine-grained sediments, the surface of leaf impressions can be distinguished by the texture of the fossil—authigenic clays are oriented parallel to the surface of the biofilm, and will remain so aligned even after organics are lost (Pan et al. 2014). This alignment in non-metamorphosed sedimentary rocks cannot be attributed to compaction, as it would affect all clay grains in a similar manner. A biofilm-clay template may also result in a distinct color in true impressions (e.g., Fig. 1D). Leaves preserved in this manner commonly exhibit a rust-color, due to the oxidation of iron within the clay matrix.

Compression fossils form by the polymerization of organic tissues into more geologically stable forms (kerogenization). Although a biofilm-clay template may not directly influence the polymerization of leaf tissues, clays are known to extend the lifespan of kerogen by providing both physical and chemical protection (Salmon et al. 2000), and may help to enhance the preservation of organic leaf compressions. Well-preserved leaf compressions usually split such that one half of the fossil retains the cohesive, often black, leaf while the other retains only an impression. Compressions exposed to oxidizing conditions in situ may retain only poorly preserved, brown organic material—but may still yield well-preserved epidermal details when examined under SEM (Harding and Chant 2000; Moisan 2012).

Three-dimensional mold-like leaf impressions form by burial in rapid, catastrophic events, such as subaqueous obrution events or overbank crevasse splays; they have greater vein relief and may cross multiple

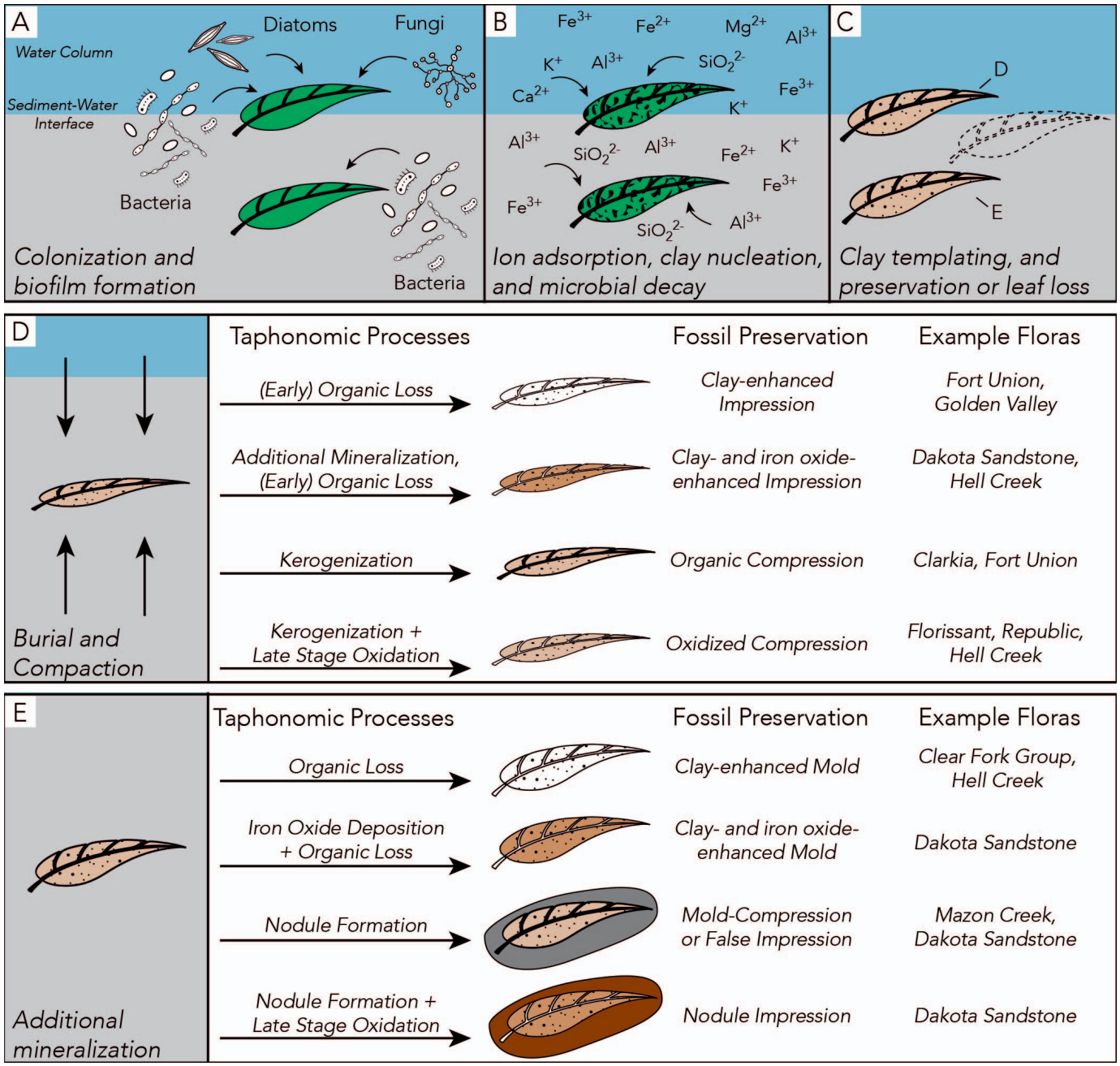

FIG. 10.—Proposed taphonomic Biofilm-Clay Template model. Upper leaf in A–C represents a leaf that decays in the water column or at the sediment water interface prior to being buried, after which it may form a flat-lying adpression through pathways outlined in D. The lower leaf in A–C represents a leaf that is rapidly buried or captured in a catastrophic burial event and may form a leaf mold through pathways outlined in E. **A**) A leaf enters the depositional environment and is colonized by microbes, including bacteria, diatoms, and fungi from the water column and sediments as well as the native leaf microflora, which excrete EPS and form a biofilm. The nature of the colonizing community will depend on the oxygen concentrations and whether the leaf is exposed to the water column (upper) or encased in sediments (lower). **B**) Dissolved metal and silicon ions adsorb onto the biofilm and form clay precursors and microbial decay progresses. **C**) Continued clay precipitation within the biofilm results in a clay template (indicated by brown color and spots). During this process, a leaf may be entirely consumed by microbial decay or consumed by detritivores (indicated by outline of leaf shape on the right). **D**) Hypothetical pathways for leaves buried slowly, resulting in flat-lying leaf adpressions of various forms. **E**) Hypothetical pathways for leaves buried rapidly, resulting in leaf molds of various forms.

bedding planes either because of curling or transport (Mamay 1989; Kauffman et al. 1990) (lower leaf Fig. 10A–10C, 10E). Leaf molds are best known from coarser-grained sediments (e.g., Dakota Sandstone), but are also occur in fine-grained sediments (e.g., Clear Fork Group, Mamay 1989). A biofilm-clay template may protect a decayed leaf during transport with fine-grained sediments, but transport with coarser grained sediments may sometimes strip the biofilm-clay template off the leaf surface and cause fragmentation.

In the Biofilm-Clay Template model, the precipitation of clay minerals is independent of the products of decay, and depends only on the formation of a suitable biofilm and the availability of metal ions in the surrounding water. This contrasts with other modes of exceptional preservation in

which authigenic mineralization is driven by the production of ions and chemical gradients by decay (such as concretion formation; Schopf 1975; Briggs 2003). Nevertheless, a biofilm-clay template may help to stabilize the surrounding sediments when formed *in situ*. Additionally, the formation of a biofilm-clay template may help to ensure leaf mold preservation in nodules oxidized late in diagenesis. Carbonates and iron oxides are prone to dissolution, recrystallization, and mineral overgrowths that may result in the loss or masking of a leaf mold, whereas aluminosilicates are less likely to be altered in a way that would decrease the quality of the fossil, particularly when bound to organic matter, such that leaves are more likely to remain distinct from the surrounding matrix.

CONCLUSIONS

The formation of leaf adpression fossils has been a phytotaphonomic mystery for decades (Schopf 1975). Previous analyses have documented the importance of microbial biofilms in fossil leaf formation (Dunn et al. 1997) but, to date, no model has explained the variation in appearance and quality exhibited by leaf adpressions, from organic-rich compressions to leaf molds in iron-rich nodules. Our analyses reveal the consistent occurrence of cation-rich aluminosilicates associated with multiple modes of leaf adpression fossilization, which our experiments strongly suggest are the result of biofilm-mediated authigenic precipitation. This is explained by a Biofilm-Clay Template model of leaf preservation, in which the early precipitation of authigenic clays on biofilm-coated leaves facilitates leaf fossilization. Future analyses of fossil leaves and leaves decaying in a wide range of environmental conditions will better characterize the clays, help to delimit the applicability of our model, and refine its details, particularly in regards to exceptional leaf compression fossils.

ACKNOWLEDGMENTS

We thank the Yale Peabody Museum of Natural History, the Paleontological Society for the James M. and Thomas J.M. Schopf Award to ERL, and the 42 backers (A. Angelo, I. Bachev, W. Broms, J. Brown, F. Coalson, C. Cope-Kasten, R. Deal, G. Effertz, K. Everaerts, H. Fuson, A. Gardner, B. and C. Garrett, M. J. Garrett, G. Giller, Z. Guri, P. Harben, S. Hardy, L. Hoff, C. Jackson, S. Kenney-Noziska, G. Kopp, K. Livermore, J. and M. Locatelli, A. Louik, R. Lower, D. Luan, J. Martínez, A. Merritt, R. Miller, C. Pelton, J. Thole, C. Warren, C. Weske, C. Wichers, M. Will, A. Wong, J. Woody, N. Zaffos, A. Zaffos, I. Zaffos) of ERL's experiment.com project "Leaves in Stone" for funding; E.J. Hodil for his assistance collecting mud and water samples; and S. Hu for his assistance in the Paleobotany Collections at the Yale Peabody Museum of Natural History. We thank D.E.G. Briggs, P.R. Crane, J.A. Gauthier, and S.L. Wing for helpful discussions about this work. The comments of M. Laflamme, R.A. Spicer, J. Peckmann and one anonymous reviewer greatly improved the manuscript. S.M. acknowledges the support of the NASA Astrobiology Institute NNA13AA90A, Foundations of Complex Life, Evolution, Preservation and Detection on Earth and Beyond.

REFERENCES

Allison, P.A., Maeda, H., Tuzino, T., and Maeda, Y., 2008, Exceptional preservation within Pleistocene lacustrine sediments of Shiobara, Japan: PALAIOS, v. 23, p. 260–266.

Anderson, E.P., Schiffbauer, J.D., and Xiao, S., 2011, Taphonomic study of Ediacaran organic-walled fossils confirms the importance of clay minerals and pyrite in Burgess Shale-type preservation: Geology, v. 39, p. 643–646.

Archibald, S.B., Greenwood, D.R., Smith, R.Y., Mathewes, R.W. and Basinger, J.F., 2011, Great Canadian Lagerstätten 1, early Eocene Lagerstätten of the Okanagan Highlands (British Columbia and Washington State): Geoscience Canada, v. 38, p. 155–164.

Beier, S., Witzel, K.P., and Marxsen, J., 2008, Bacterial community composition in Central European running waters examined by temperature gradient gel electrophoresis and sequence analysis of 16S rRNA genes: Applied and Environmental Microbiology, v. 74, p. 188–199.

Bontognali, T.R., Martinez-Ruiz, F., McKenzie, J.A., Bahniuk, A., Anjos, S., and Vasconcelos, C., 2014, Smectite synthesis at low temperature and neutral pH in the presence of succinic acid: Applied Clay Science, v. 101, p. 553–557.

Briggs, D.E.G., 2003, The role of biofilms in the fossilization of non-biomineralized tissues, *in* W.E. Krumbein, D.M. Paterson, and G.A. Zavarzin (eds.), Fossil and Recent Biofilms: A Natural History of Life on Earth: Kluwer Academic Publishers, Dordrecht, p. 281–290.

Burnham, R.J., 1996, Republic leaf deposits and Eocene ecology: Washington Geology, v. 24, p. 19.

Butterfield, N.J., Balthasar, U., and Wilson, L.A., 2007, Fossil diagenesis in the Burgess Shale: Palaeontology, v. 50, p. 537–543.

Cai, Y., Schiffbauer, J.D., Hua, H., and Xiao, S.H., 2012, Preservational modes in the Ediacaran Gaijiashan Lagerstätte: pyritization, aluminosilicification, and carbonaceous compression: Palaeogeography, Palaeoclimatology, Palaeoecology, v. 326-328, p. 109–117.

Das, M., Royer, T.V., and Leff, L.G., 2007, Diversity of fungi, bacteria, and actinomycetes on leaves decomposing in a stream: Applied and Environmental Microbiology, v. 73, p. 756–767.

Dunn, K.A., McLean, R.J.C., Upchurch, G.R., and Folk, R.L., 1997, Enhancement of leaf fossilization potential by bacterial biofilms: Geology, v. 25, p. 1119–1122.

Farley, M.B. and Dilcher, D.L., 1986, Correlation between miospores and depositional environments of the Dakota Formation (mid-Cretaceous) of north-central Kansas and adjacent Nebraska, USA: Palynology, v. 10, p. 117–133.

Ferris, F.G., Tazaki, K., and Fyfe, W.S., 1989, Iron oxides in acid mine drainage environments and their association with bacteria: Chemical Geology, v. 74, 3, p. 321–330.

Forchielli, A., Steiner, M., Kasbohm, J., Hu, S., and Keupp, H., 2014, Taphonomic traits of clay-hosted early Cambrian Burgess Shale-type fossil Lagerstätten in South China: Palaeogeography, Palaeoclimatology, Palaeoecology, v. 398, p. 59–85.

Gabbott, S., Norry, M., Aldridge, R., and Theron, J., 2001, Preservation of fossils in clay minerals; a unique example from the Upper Ordovician Soom Shale, South Africa: Proceedings of the Yorkshire Geological Society, v. 53, p. 237–244.

Gaines, R.R., Briggs, D.E.G., and Yuanlong, Z., 2008, Cambrian Burgess Shale-type deposits share a common mode of fossilization: Geology, v. 36, p. 755–758.

Gallardo, A. and Merino, J., 1993, Leaf decomposition in two Mediterranean ecosystems of southwest Spain. influence of substrate quality: Ecology, v. 74, p. 152–161.

Glasauer, S., 2011, Nanocrystals, Microbially Induced, *in* J. Reitner and V. Thiel (eds.), Encyclopedia of Geobiology: Springer Netherlands, Dordrecht, p. 681–684.

Harding, I.C. and Chant, L.S., 2000, Self-sedimented diatom mats as agents of exceptional fossil preservation in the Oligocene Florissant lake beds, Colorado, United States: Geology, v. 28, p. 195–198.

Hedges, J.I. and Keil, R.G., 1995, Sedimentary organic matter preservation: an assessment andspeculative synthesis: Marine Chemistry, v. 49, p. 81–115.

Johnson, K.R., 2002, Megaflora of the Hell Creek and lower Fort Union Formations in the western Dakotas: vegetational response to climate change, the Cretaceous–Tertiary boundary event, and rapid marine transgression: Geological Society of America Special Paper, v. 361, p. 329–391.

Kauffman, E.G., Upchurch, G.R., and Nichols, D.J., 1990, The Cretaceous–Tertiary boundary interval at south table mountain, near Golden, Colorado, *in* E.G. Kauffman and O.H. Walliser (eds.), Extinction Events in Earth History, Proceedings of the Project 216: Global Biological Events in Earth History: Springer, Berlin Heidelberg, p. 365–392.

Kawano, M. and Tomita, K., 2001, Microbial biomineralization in weathered volcanic ash deposit and formation of biogenic minerals by experimental incubation: American Mineralogist, v. 86, p. 400–410.

Kok, C.J. and Velde, G.V.D., 1994, Decomposition and macroinvertebrate colonization of aquatic and terrestrial leaf material in alkaline and acid still water: Freshwater Biology, v. 31, p. 65–75.

Konhauser, K.O., Fisher, Q., Fyfe, W., Longstaffe, F., and Powell, M., 1998, Authigenic mineralization and detrital clay binding by freshwater biofilms: the Brahmani River, India: Geomicrobiology Journal, v. 15, p. 209–222.

Konhauser, K.O., Fyfe, W., Ferris, F., and Beveridge, T., 1993, Metal sorption and mineral precipitation by bacteria in two Amazonian river systems: Rio Solimões and Rio Negro, Brazil: Geology, v. 21, p. 1103–1106.

Konhauser, K.O., 1998, Diversity of bacterial iron mineralization: Earth-Science Reviews, v. 43, p. 91–121.

Konhauser, K.O., 2011, Clay Authigenesis, Bacterial, *in* J. Reitner and V. Thiel (eds.), Encyclopedia of Geobiology: Springer Netherlands, Dordrecht, p. 274–277.

Konhauser, K.O. and Urrutia, M.M., 1999, Bacterial clay authigenesis: a common biogeochemical process: Chemical geology, v. 161, p. 399–413.

Laflamme, M., Schiffbauer, J.D., Narbonne, G.M., and Briggs, D.E.G., 2011, Microbial biofilms and the preservation of the Ediacara biota: Lethaia, v. 44, p. 203–213.

Leopold, E.B., Updegrave, C.A., and Maier, K., 1996, Pollen and spores characteristic of Eocene sediments at Republic, Washington: Washington Geology, v. 24, p. 28.

Locatelli, E.R., 2013, The exceptional preservation of leaves in iron-rich sediments from Oceania: Geological Society of America Abstracts with Programs, v. 47, p. 455.

Locatelli, E.R., 2014, The exceptional preservation of plant fossils: a review of taphonomic processes and biases in the fossil record, *in* M. Laflamme, J.D. Schiffbauer, and S.A.F. Darroch (eds.), Reading and Writing of the Fossil Record: Preservational Pathways to Exceptional Fossilization: Paleontological Society Papers, p. 237–258.

Locatelli, E.R., Krajewski, L., Chochinov, A.V., and Laflamme, M., 2016, Taphonomic variance between marattialean ferns and medullosan seed ferns in the Carboniferous Mazon Creek Lagerstätte, Illinois, USA: PALAIOS, v. 31, p. 97–110.

Mamay, S.H., 1989, *Evolsonia*, a new genus of Gigantopteridaceae from the Lower Permian Vale Formation, north-central Texas: American Journal of Botany, v. 76, p. 1299–1311.

McLean, R., Fuqua, C., Siegele, D., Kirkland, B., Adams, J., and Whiteley, M., 1999, Biofilm growth and illustrations of its role in mineral formation, *in* C.R. Bell, M. Brylinsky, and P. Johnson-Green (eds.), Microbial Biosystems: New Frontiers: Proceedings of the 8th International Symposium on Microbial Ecology: Atlantic Canada Society for Microbial Ecology, Halifax, Canada, p. 255–261.

McNamara, C.J. and Leff, L.G., 2004, Bacterial community composition in biofilms on leaves in a northeastern Ohio stream: Journal of the North American Benthological Society, v. 23, p. 677–685.

McNamara, M.E., Briggs, D.E.G., and Orr, P.J., 2012, The controls on the preservation of structural color in fossil insects: PALAIOS, v. 27, p. 443–454.

Meyer, H.W., 2003, The Fossils of Florissant: Smithsonian Books, Smithsonian Institution, Washington, DC, 258 p.

Meyer, J. L., Wallace, J. B., and Eggert, S. L., 1998, Leaf litter as a source of dissolved organic carbon in streams: Ecosystems, v. 1, p. 240–249.

Meyer, M., Schiffbauer, J.D., Xiao, S., Cai, Y., and Hua, H., 2012, Taphonomy of the upper Ediacaran enigmatic ribbonlike fossil *Shaanxilithes*: PALAIOS, v. 27, p. 354–372.

Michalopoulos, P. and Aller, R.C., 2004, Early diagenesis of biogenic silica in the Amazon delta: alteration, authigenic clay formation, and storage: Geochimica et Cosmochimica Acta, v. 68, p. 1061–1085.

Mikutta, R., Zang, U., Chorover, J., Haumaier, L., and Kalbitz, K., 2011, Stabilization of extracellular polymeric substances (*Bacillus subtilis*) by adsorption to and coprecipitation with Al forms: Geochimica et Cosmochimica Acta, v. 75, p. 3135–3154.

Moisan, P., 2012, The study of cuticular and epidermal features in fossil plant impressions using silicone replicas for scanning electron microscopy: Palaeontologia Electronica, v. 15, 15.2.23A.

Morris, C.E., Monier, J., and Jacques, M., 1997, Methods for observing microbial biofilms directly on leaf surfaces and recovering them for isolation of culturable microorganisms: Applied and Environmental Microbiology, v. 63, p. 1570–1576.

Moss, P.T., Greenwood, D.R., and Archibald, S.B., 2005, Regional and local vegetation community dynamics of the Eocene Okanagan Highlands (British Columbia Washington State) from palynology: Canadian Journal of Earth Sciences, v. 42, p. 187–204.

Mustoe, G.E., 2005, Diatomaceous origin of siliceous shale in Eocene lake beds of central British Columbia: Canadian Journal of Earth Sciences, v. 42, p. 231–241.

O'Brien, N.R., Meyer, H.W., and Harding, I.C., 2008, The role of biofilms in fossil preservation, Florissant Formation, Colorado: Geological Society of America Special Papers, v. 435, p. 19–31.

Pacton, M., Fiet, N., and Gorin, G.E., 2007, Bacterial activity and preservation of sedimentary organic matter: the role of exopolymeric substances: Geomicrobiology Journal, v. 24, p. 571–581.

Page, A., Gabbott, S.E., Wilby, P.R., and Zalasiewicz, J.A., 2008, Ubiquitous Burgess Shale-style "clay templates" in low-grade metamorphic mudrocks: Geology, v. 36, p. 855–858.

Pan, Y., Sha, J., and Fuersich, F.T., 2014, A model for organic fossilization of the Early Cretaceous Jehol Lagerstätte based on the taphonomy of "*Ephemeropsis trisetalis*": PALAIOS, v. 29, p. 363–377.

Peppe, D., Evans, D., and Smirnov, A., 2009, Magnetostratigraphy of the Ludlow Member of the Fort Union Formation (lower Paleocene) in the Williston Basin, North Dakota: Geological Society of America Bulletin, v. 121, p. 65–79.

Potter-McIntyre, S., Chan, M., and McPherson, B.J., 2014, Concretion formation in volcaniclastic host rocks: evaluating the role of organics, mineralogy, and geochemistry on early diagenesis: Journal of Sedimentary Research, v. 84, p. 875–892.

Ravn, R.L. and Witzke, B.J., 1994, The mid-Cretaceous boundary in the Western Interior Seaway, central United States: implications of palynostratigraphy from the type Dakota Formation: Geological Society of America Special Papers, v. 287, p. 111–128.

Retallack, G. and Dilcher, D., 2012, Core and geophysical logs versus outcrop for interpretation of Cretaceous paleosols in the Dakota Formation of Kansas: Palaeogeography, Palaeoclimatology, Palaeoecology, v. 329, p. 47–63.

Rex, G.M. and Chaloner, W.G., 1983, The experimental formation of plant compression fossils: Palaeontology, v. 26, p. 231–252.

Rex, G.M., 1986, Further experimental investigations on the formation of plant compression fossils: Lethaia, v. 19, p. 143–159.

Salmon, V., Derenne, S., Lallier-Verges, E., Largeau, C., and Beaudoin, B., 2000, Protection of organic matter by mineral matrix in a Cenomanian black shale: Organic Geochemistry, v. 31, p. 463–474.

Schopf, J.M., 1975, Modes of fossil preservation: Review of Palaeobotany and Palynology, v. 20, p. 27–53.

Shute, C.H. and Cleal, C.J., 1986, Palaeobotany in museums: Geological Curator, v. 4, p. 553–559.

Souza-Egipsy, V., Wierzchos, J., Ascaso, C., and Nealson, K.H., 2005, Mg-silica precipitation in fossilization mechanisms of sand tufa endolithic microbial community, Mono Lake (California): Chemical Geology, v. 217, p. 77–87.

Spicer, R.A., 1977, The pre-depositional formation of some leaf impressions: Palaeontology, v. 20, p. 907–912.

Urrutia, M.M. and Beveridge, T.J., 1994, Formation of fine-grained metal and silicate precipitates on a bacterial surface (*Bacillus subtilis*): Chemical Geology, v. 116, p. 261–280.

Vorhies, J.S. and Gaines, R.R., 2009, Microbial dissolution of clay minerals as a source of iron and silica in marine sediments: Nature Geoscience, v. 2, doi:10.1038/ngeo441.

Wacey, D., Saunders, M., Roberts, M., Menon, S., Green, L., Kong, C., Culwick, T., Strother, P., and Brasier, M.D., 2014, Enhanced cellular preservation by clay minerals in 1 billion-year-old lakes: Scientific Reports, v. 4, article 5841.

Webster, J. and Benfield, E., 1986, Vascular plant breakdown in freshwater ecosystems: Annual Review of Ecology and Systematics, v. 17, p. 567–594.

Westall, F., Steele, A., Toporski, J., Walsh, M., Allen, C., Guidry, S., McKay, D., Gibson, E., and Chafetz, H., 2000, Polymeric substances and biofilms as biomarkers in terrestrial materials: implications for extraterrestrial samples: Journal of Geophysical Research. Planets, v. 105, p. 24511–24527.

Wilson, L.A. and Butterfield, N.J., 2014, Sediment effects on the preservation of Burgess Shale-type compression fossils: PALAIOS, v. 29, p. 145–154.

Wright, M. and Covich, A., 2005, Relative importance of bacteria and fungi in a tropical headwater stream: leaf decomposition and invertebrate feeding preference: Microbial Ecology, v. 49, p. 536–546.

Received 16 May 2017; accepted 29 October 2017.